Unpublished data has been removed in this e-publication.

Towards Anti-Virulence Antimicrobials

Discovery and Development of Sortase A Inhibitors and Investigations of Bacterial Phenotypes

PATRICK M. WEHRLI

UNIVERSITY OF GOTHENBURG

Department of Chemistry and Molecular Biology
University of Gothenburg
2016

DOCTORAL THESIS

Submitted for fulfilment of the requirements for the degree of
Doctor of Philosophy in Chemistry

Towards Anti-Virulence Antimicrobials
Discovery and Development of Sortase A Inhibitors and Investigations of Bacterial Phenotypes

PATRICK M. WEHRLI

ISBN: 978-91-628-9906-6
http://hdl.handle.net/2077/45837

Department of Chemistry and Molecular Biology
SE-412 96 Göteborg
Sweden

Printed by Ineko AB
Kållered, 2016

Unpublished data has been removed in this e-publication.

To my grandfathers

Abstract

Antibiotic resistance is an emerging and serious threat to public health. Immediate actions are required to preserve current antibiotics while intensifying research efforts towards the development of new effective therapeutics. A novel approach to combat bacterial infections focuses on the inhibition of bacterial virulence to inhibit disease-causing properties rather than bacterial growth. In several Gram-positive bacteria, the bacterial enzyme sortase A (SrtA) is critical for an intact cell surface display of virulence-associated proteins. Inhibition of SrtA is, therefore, expected to greatly reduce bacterial virulence, serving as a potential therapeutic approach to treat Gram-positive infections. In order to fully exploit novel intervention strategies we need to further improve our understanding of bacterial virulence, persistence and stress responses.

Firstly, this thesis describes the discovery, synthesis and evaluation of inhibitors of SrtA. Secondly, the phenotypic characterization of bacteria using Fourier-transform infrared (FTIR) spectroscopy as well as time-of-flight secondary ion mass spectrometry (ToF-SIMS) is discussed.

A new class of SrtA inhibitors was identified by high-throughput screening of ~28500 small-molecule compounds. Synthetic modification of hit structures yielded a series of compounds that exhibited increased inhibitory activity in a functional, FRET based, assay. Ligand-detected protein binding experiments using Carr-Purcell-Meiboom-Gill (CPMG) relaxation dispersion NMR spectroscopy confirmed binding to SrtA and guided the design of new structures. The reversibility of binding, binding kinetics, and binding affinity were determined by surface plasmon resonance (SPR) spectroscopy. All compounds tested displayed a reversible binding mode and some exhibited a very high binding affinity.

In a feasibility study, FTIR spectroscopy in combination with design of experiment and multivariate statistical analysis (MVA) was applied to explore the condition dependent phenotypic diversity of *Staphylococcus aureus*. Planktonic cultures of *S. aureus* were grown under various conditions according to the experimental design. FTIR spectra obtained from each treatment group contained distinct profiles that allowed full cluster separation in principal components analysis (PCA).

ToF-SIMS was employed for further and more detailed characterization of bacterial phenotypes by direct analysis of native cell samples. Initial experiments demonstrated the capability of ToF-SIMS, coupled with MVA, to fully differentiate *Escherichia coli*, *Pseudomonas aeruginosa*, as well as two strains of *S. aureus*. Further investigations focused more specifically on *E. coli* and explored the role of the stringent response in growth phase dependent lipid modifications. Mass spectral assignments revealed that a $ppGpp^0$ mutant exhibited alterations in lipid composition in stationary phase. Results suggest the occurrence of alternative stress response mechanisms that are regulated independently of ppGpp.

Keywords: Sortase A, SrtA, Inhibitors, Anti-virulence, Bacterial analysis, FTIR spectroscopy, Bacterial phenotyping, Design of Experiment, Multivariate Data Analysis, PCA, ToF-SIMS, Time-of-flight secondary-ion-mass-spectrometry, Lipid analysis, ppGpp, Stringent response.

List of Publications

This thesis is based on the following publications, which are referred to in the text by the Roman numerals **I–IV**.

I **Discovery and development of inhibitors of *Staphylococcus aureus* sortase A**
Patrick M. Wehrli, Ivana Uzelac, Tomas Jacso, Thomas Olsson, and Johan Gottfries
Manuscript

II **Exploring bacterial phenotypic diversity using factorial design and FTIR multivariate fingerprinting**
Patrick M. Wehrli, Erika Lindberg, Olof Svensson, Anders Sparén, Mats Josefson, R. Hugh Dunstan, Agnes E. Wold and Johan Gottfries
Journal of Chemometrics **2014***, 28,* S681–S686.

III **Maximising the potential for bacterial phenotyping using time-of-flight secondary ion mass spectrometry with multivariate analysis and Tandem Mass Spectrometry**
Patrick M. Wehrli, Erika Lindberg, Tina B. Angerer, Agnes E. Wold, Johan Gottfries and John S. Fletcher
Surface and Interface Analysis **2014**, *46* (S1), 173-176.

IV **Investigating the role of the stringent response in lipid modifications during the stationary phase in *E. coli* by direct analysis with ToF-SIMS**
Patrick M. Wehrli, Tina B. Angerer, Anne Farewell, John S. Fletcher, and Johan Gottfries
Analytical Chemistry **2016**.

The Author's Contribution to Papers I–IV

I Formulated the research problem, performed the major part of the experimental work, interpreted the results, and wrote the manuscript.

II Contributed to the formulation of the research problem, performed all experimental work, contributed considerably to the interpretation of the results, and wrote the manuscript.

III Contributed significantly to the formulation of the research problem, performed the major part of the experimental work, interpreted the results, and wrote the major part of the manuscript.

IV Formulated the research problem, performed the major part of the experimental work, interpreted the results, and wrote the manuscript.

List of Abbreviations

AAEK	Aryl(*β*-amino)ethyl ketone
Arg	Arginine
ATR	Attenuated total reflectance
cam	Chloramphenicol
CDC	Centre for Disease Control and Prevention
Cfa	Cyclopropane fatty acid synthase
cfa	Gene, encoding cyclopropane fatty acid synthase
CID	Collision induced dissociation
CL	Cardiolipin
Cls	Cardiolipin synthase
cp	Cyclopropane
CPMG	Carr-Purcell-Meiboom-Gill
CV	Cross validation
Cys	Cysteine
DNA	Deoxyribonucleic acid
DoE	Design of experiments
EPEC	Enteropathogenic *E. coli*
FA	Fatty acid
FAME	Fatty acid methyl ester
FRET	Fluorescence resonance energy transfer
FTIR	Fourier transform infrared
GC/MS	Gas chromatography/mass spectrometry
GCIB	Gas cluster ion beam
Gly	Glycine
HAQs	4-hydroxy-2-alkylquinolines
His	Histidine
HTS	High-throughput screening
IC_{50}	Half maximal inhibitory concentration
kan	Kanamycin
K_D	Equilibrium dissociation constant
LB	Lysogeny broth
m/z	Mass to charge ratio
MALDI	Matrix assisted laser desorption ionization
MIC	Minimum inhibitory concentration
MLR	Multiple linear regression
MRSA	Methicillin-resistant *S. aureus*
MSC	Multiplicative scatter correction
MSCRAMMs	Microbial Surface Components Recognizing Adhesive Matrix Molecules
MSMS	tandem mass spectrometry
MVA	Multivariate Data Analysis
n.a.	Not applicable

NMR	Nuclear magnetic resonance
OD	Optical density
OPLS	Orthogonal partial least squares projections to latent structures
OSC	Orthogonal signal correction
PA	Phosphatidic acid
PC	Principal component
PCA	Principal components analysis
PD	Pharmacodynamics
PE	Phosphatidylethanolamine
PG	Phosphatidylglycerol
PK	Pharmacokinetics
ppGpp	Guanosine tetraphosphate
$ppGpp^0$	ppGpp-deficient mutant
Q^2	Model predictability value
QS	Quorum sensing
R^2	Model explanation value
relA	Gene, coding for ppGpp synthetases I
RelA	ppGpp synthetase I
SAR	Structure-activity relationship
SD	Standard deviation
SG	Savitzky-Golay (smoothing)
SIMS	Secondary ion mass spectrometry
SNV	Standard normal variate transformation
spoT	Gene, coding for ppGpp synthetases II
SpoT	ppGpp synthetase II
SPR	Surface Plasmon Resonance
srtA	Gene, coding for Sortase A
SrtA	Sortase A protein
T3SS	Type III secretion system
Thr	Threonine
ToF	Time-of-flight
UV	Unit variance (scaling)
WHO	World Health Organization

Table of Contents

1 INTRODUCTION

1.1 The Global Threat of Antimicrobial Resistance

The emergence of bacterial pathogens that are resistant to current antimicrobial therapies and the continuous spreading of their resistance genes constitute a serious threat to public health.[1] With a shortage of effective therapeutic options, multidrug resistance presents one of our greatest challenges in combat against bacterial infections and associated diseases.[2] To avert a global health crisis, actions across all government sectors and society are urgently needed.[3, 4]

Traditional approaches for the treatment and prevention of bacterial infections rely on the inhibition of bacterial growth by disrupting crucial bacterial processes such as cell wall synthesis, DNA replication, or protein synthesis.[5] Antibiotics that inhibit growth by bacteriostatic (reversible inhibition of growth) or bactericidal (killing bacteria) actions exert a substantial evolutionary selection pressure which favors the selection for resistant subpopulations. Many of the antimicrobials available today are derived from natural compounds that originate from antibiotic-producing microorganisms. It is very likely that antibiotics and their resistance genes have evolved naturally for millions of years and existed long before their discovery.[6, 7] The inappropriate and excessive human use of antibiotics, however, has unnaturally accelerated the evolutionary process contributing to the emergence of pathogens that are highly resistant to the majority of antibiotics currently available.[2] Furthermore, the mismanagement of antibiotics, particularly for non-curative purposes such as prophylaxis, metaphylaxis, and growth promotion in animal feed stocks has also exacerbated the global spread of resistance.[2]

The World Health Organization (WHO) has recognized antimicrobial resistance as one of the greatest threats to public health, with a post-antibiotic era as a real possibility for the 21st century.[1] In the European Union, drug-resistant bacteria alone are estimated to cause 25000 deaths with healthcare and socioeconomical costs amounting to EUR 1.5 billion each year.[8] Similarly, the Centers for Disease Control and Prevention (CDC) estimates that in the USA more than 2 million infections and 23000 deaths annually are caused by antibiotic-resistant bacteria.[9] The current situation requires immediate actions at all societal levels to reduce the impact and spread of resistance. Synergistic actions of preserving the drugs at hand while intensifying research efforts towards the development of new therapeutics may be key to avert a global health crisis. In 2015, the WHO released a global action plan[3] with the following strategic objectives that '*aim to ensure that the prevention and treatment of infectious diseases with safe and effective medicines continues*':

- improving awareness of antimicrobial resistance
- strengthening surveillance and research
- reducing the incidence of infection
- optimizing the use of antibiotics
- ensuring sustainable investment in countering antimicrobial resistance

The continuous increase in antibiotic resistant infections creates a strong need for novel effective therapies. The shortage of new antibiotics coming to market is associated with limited interests of pharmaceutical companies in the development of antimicrobial drugs. This lack of interest is the result of antibiotic management policies that limit the return of investment.[2, 10] Companies may be stimulated to increase their efforts in the development new therapies by initiating policy changes, creating incentives, and lowering regulatory hurdles.

Novel intervention strategies need to respond to current antimicrobial resistance and preferably circumvent selection pressure, which otherwise may again result in the onset of drug resistance.

1.2 Bacterial Resistance, Tolerance, and Persistence

Bacteria have evolved a number of strategies by which they can survive a number of environmental challenges, including antibiotic exposure. These survival strategies have been described and differentiated using the terms 'resistance', 'tolerance' and 'persistence' despite a certain ambiguity.[11, 12]

1.2.1 Resistance

Bacterial resistance to antibiotics is typically associated with inheritable resistance traits which involve molecular mechanisms that allow bacteria to continue to proliferate in the presence of high concentrations of antibiotics.[12] These mechanisms are conferred by resistance genes and can be acquired and spread by horizontal gene transfer or developed by adaptive mutations. Resistance can arise due to (i) genetically mutated or post-translationally modified antibiotic targets, (ii) antibiotic efflux systems that reduce intracellular antibiotic concentration, or (iii) the ability to deactivate drug molecules by hydrolysis or structural modification.[4, 12] In addition, the absence of a susceptible target or the inability of drugs to cross the cell envelope may confer intrinsic resistance.[2, 6]

1.2.2 Tolerance

Bacterial tolerance to antibiotics usually refers to the ability of the microorganisms to survive a transient exposure to normally lethal concentrations of bactericidal antibiotics.[11, 12] The mode of action of numerous antibiotics requires bacteria to be in an active metabolic state of growth. Tolerance to such antibiotics is associated with strongly reduced growth

rates.[11] Various environmental conditions, including starvation stress, can induce phenotypic adaptations and metabolic adjustments that lead to slow growth or growth arrest.[13-15] This can render phenotypic variants of an otherwise antibiotic-sensitive strain drug-tolerant. In contrast to resistance, tolerance is a transient phenomenon, which is not based on resistance genes. It also affects several classes of antibiotics rather than one specific class as found in bacterial resistance (except in cases involving multidrug resistance).

1.2.3 Persistence

Another bacterial survival strategy is based on the phenotypic heterogeneity of a bacterial population. Phenotypic heterogeneity is a phenomenon of evolutionary adaptation that promotes bacterial persistence under environmental insults.[16] A clonal bacterial population exhibits a small fraction of persister cells (genetically identical phenotypic variant of typically less than 1%) that stochastically enter a state of slow growth, rendering them tolerant to antibiotics.[17, 18] This subpopulation of persister cells is therapy-refractive and therefore presents a primary source for chronic and relapsing infections.[19] Molecular mechanisms that lead to persistence and drug tolerance are often linked to the signaling molecule, ppGpp. Such mechanisms include toxin-antitoxin (TA) systems that reduce metabolic activity in response to stresses in fluctuating environments.[20, 21] Persister formation may also be modulated by quorum sensing (QS), a bacterial communication phenomenon based on chemical signaling.[22] The above mentioned systems are also associated with the formation of biofilms, multilayered bacterial communities, which may provide further protection against attacks from antibiotics and the host immune system.[21]

1.3 Anti-Virulence Strategies to Combat Bacterial Infections

As previously mentioned, the increasing threat of antimicrobial resistance demands the development of new therapeutics and alternative intervention strategies. An increasing amount of research effort has been devoted to strategies that are based on the inhibition of bacterial virulence.[5, 23, 24] In this thesis, bacterial virulence refers to the quantitative capacity of a bacterium to infect and cause disease in host organisms.[25] Bacterial virulence is dynamically regulated in response to environmental cues, such as conditions and signaling, and its extent may be dependent on a pathogen's ability to multiply within the host.[24, 26] Anti-virulence strategies focus on the interference with virulence associated mechanisms to confer inhibition to disease causing properties without killing the bacteria. As a consequence, this strategy might exert a milder evolutionary pressure for drug-resistant selection and lead to fewer undesirable effects to the host microbiota that are associated with traditional strategies.[5, 24] Anti-virulence drugs may allow the host immune system to contain and clear the infection, and could alternatively be administered in a combination therapy with available antibiotics.[5, 24]

Numerous anti-virulence strategies are currently under investigation. These include targeting bacterial adhesion, invasion and biofilms, interfering with bacterial signaling and gene regulation systems, as well as inhibiting toxin function and specialized secretion systems. The following sections aim to highlight some of the major anti-virulence approaches that are being developed.

1.3.1 Targeting Adhesion and Biofilms

Bacterial adhesion to host cells is critical for the initiation of the infection process and to effectively colonize the host. Adhesion usually involves direct and specific interactions between bacterial surface proteins (adhesins) and receptors on the host cells.[27] Most bacteria will only infect specific hosts and host tissues that present corresponding receptors.[5] Gram-negative bacteria most commonly exhibit adhesins incorporated in filamentous surface structures called pili or fimbriae, however, some bacteria express adhesins also in monomeric forms or complexes.[24, 28, 29] Gram-positive bacteria feature Microbial Surface Components Recognizing Adhesive Matrix Molecules (MSCRAMMs) that are associated with virulence and biofilm formation.[30, 31] Attachment to host cells enables bacteria to avoid mechanical removal or clearance by the host immune system and further promotes the formation of biofilms.[27] Moreover, contact is required for the activation of specific toxin secretion systems and for toxins that depend on certain local toxin concentrations in order to be effectively active.[32]

Anti-virulence strategies that aim to inhibit bacterial adhesion may limit the interaction between bacteria and host cell early on in the infection process and in turn, reduce the risk for the establishment of infections.[24, 33] Decreased surface adhesion and biofilm formation would render bacteria less protected against antibiotic exposure and clearance by phagocytosis.[34] Furthermore, it may prevent the activation of toxin secretion systems and the release of host cell damaging factors.[32] Ideally, inhibition of adhesion would not affect *in vitro* growth and thus, exert only a low pressure for drug resistant selection. Therefore, inhibition of adhesion and biofilm formation may be an effective strategy to prevent and combat bacterial infections.

Anti-adhesion strategies may include direct inhibition of adhesins, their presentation on the cell surface, or assembly of bacterial surface structures that effect adhesion. For example, bicyclic 2-pyridones were discovered to inhibit the formation of pili in uropathogenic *Escherichia coli*. As a result of reduced pilus formation, these '*pilicides*' effected significantly reduced bacterial adherence to bladder cells, and biofilm formation.[35] Gram-positive bacteria, such as *Staphylococcus aureus*, use sortase enzymes to attach proteins and assemblies (including adhesins and pili) to the cell wall for surface display.[33] Specifically, sortase A (SrtA) was found to be essential for bacterial virulence and therefore presents a potential anti-virulence target to prevent adhesion and biofilm formation (SrtA is further discussed in *Section 3.1*). Further strategies that specifically target biofilms may prevent their formation or lead to their

resolution.[5] Quorum sensing plays an important role in the control of biofilm formation and virulence.[36] Therefore, it serves as a valuable target for anti-virulence therapy, which is discussed further in the following section.

1.3.2 Targeting Signaling and Regulation

Bacteria carefully control the expression of their virulence factors in efforts to optimize energy expenditure.[5] Virulence gene expression is regulated at various levels and implicates complex regulatory networks. Thereby, numerous mechanisms are involved, which often rely on sensing environmental signals.[24] These signals can arise from conditions, such as nutrient availability, or from other bacteria that use chemical signaling for quorum sensing (QS).[5] Various nutritional stress cues may trigger the stringent response (i.e. a global stress response), which is, among other things, implicated in the regulation of virulence. The stringent response is discussed in detail in *Section 5.3.1*. In QS, bacteria release QS signaling molecules into their surrounding environment, which accumulate upon bacterial population growth. QS systems allow bacteria to sense cell density in order to respond with appropriate adjustments in gene expression that effect regulation of bacterial virulence traits.[37] For example, *Pseudomonas aeruginosa* uses two groups of chemical signals, acyl homoserine lactones (AHLs) and the 4-quinolones, also referred to as *Pseudomonas* quinolone signal.[5] These are involved in several quorum-sensing mechanisms that regulate the expression of an array of virulence traits including adhesins, proteases, toxin secretion systems and the formation of biofilms.[24, 38] The Gram-positive bacterium *S. aureus* regulates its virulence gene expression *via* the two-component Agr QS system, involving autoinducing peptides (AIPs) that function as QS signaling molecules. These AIPs bind to histidine sensor kinase (AgrC) in the bacterial membrane, which as a result, activates a response regulator (AgrA). The response regulator, AgrA, is usually a transcription factor responsible for the stimulation of gene transcription, which finally leads to the expression of virulence factors.[24]

Due to its pivotal role in the expression of virulence traits, QS is the focus of many anti-virulence strategies that attempt to exploit signaling pathways as therapeutic targets.[39] Strategies that target QS may interfere in various mechanisms in underlying pathways for example, inhibition of signal synthesis, inhibition of signal binding to AgrC, or degradation of signal molecules (quorum quenching).[29] QS systems are not usually found in eukaryotic host cells and in summary makes QS an attractive target for pharmacological intervention.[5]

Interfering with QS may reduce bacterial virulence with therapeutic effect. QS mutants of various types of bacteria were found to exhibit reduced virulence *in vivo*.[5] Further, a small molecule inhibitor of QS, C-30, was found to be efficacious in a mouse pulmonary infection model against *P. aeruginosa* as a result of inhibited virulence factor expression.[40] An example of interference with the Agr system of *S. aureus* presents Solonamide B, a natural compound isolated from marine microorganisms. Solonamide B interfered competitively with AIP

binding to the AgrC receptor, which led to strong reduction in virulence as a result of decreased toxin activity (α-hemolysin, phenol-soluble modulins).[41, 42]

1.3.3 Targeting Toxins and Secretion Systems

Numerous bacterial species exhibit toxins and sophisticated secretion systems with which they fight competitors and acquire nutrients with various, but mostly damaging, effects to their host.[43-45] Tissue damage and cellular malfunctions are caused by exotoxins and effectors, and give rise to serious disease symptoms of, for example, anthrax disease.[46] Exotoxins are virulence factors that are excreted into the extracellular environment where they can directly act on host cells and inhibit cellular functions. Most exotoxins are pore-forming proteins, capable of oligomerizing and inserting into the membrane of the host cell to form a transmembrane pore, which potentially leads to cell death.[47] Effectors, on the other hand, are proteins that are injected into the host cell cytoplasm *via* specialized secretion systems. There, they modulate host cell functions by interfering in signaling pathways to promote the disease process.[5] There are three types of secretion systems (type III, IV, and VI) that are known to mediate the translocation of bacterial effectors.[5] The type III secretion system (T3SS) is a multi-protein assembly with a needle-like structure that crosses the bacterial cell envelope.[24, 48] The T3SS is conserved between different bacteria and has shown to be essential for the virulence of many Gram-negative pathogens such as *P. aeruginosa*, *E. coli*, *Salmonella* spp., *Shigella* spp., and *Chlamydia* spp.[29, 39, 48]

Toxins and effectors are maybe the most obvious mediators of bacterial virulence and thus, are the focal point of multiple anti-virulence strategies. These strategies target the synthesis, the activity, and trafficking pathways of exotoxins by competitive inhibition or neutralizing antibodies.[5, 49] Furthermore, inhibition of effector translocation by interfering with secretion systems (such as T3SS) may prevent damage to the host and the progression of the disease.[48]

Aurodox, a linear polyketide compound, was found to selectively inhibit T3SS-mediated hemolysis and effector secretion (EspB, EspF and Map) without affecting bacterial growth *in vitro*. *In vivo* studies demonstrated that the use of aurodox contributed to the survival of mice infected with *Citrobacter rodentium*, which was used as model strain for human pathogens, such as enteropathogenic *E. coli* (EPEC).[50] An example for an anti-virulence strategy targeting exotoxin synthesis is given by the small-molecule compound virstatin. By interfering with the homodimerization of the transcription factor, ToxT, in *Vibrio cholera*, virstatin prevents the expression of cholera toxin and the toxin co-regulated pilus. As a result, virstatin protected mice from intestinal colonization by *V. cholerae*.[51] Unfortunately, bacterial resistance to virstatin, arising from a single nucleotide polymorphism in ToxT, has already been observed.[51]

1.3.4 Potential and Limitations

Research directed towards anti-virulence therapies has produced promising evidence suggesting that the inhibition of virulence may prove to be an effective strategy to prevent and combat bacterial infections.[5, 24, 29, 39] Anti-virulence therapy may enable the normal host immune response to contain and clear the infection, and may also be coupled with the use of commercially available antibiotics.[5] This approach may have synergistic therapeutic effects and extend the effective life-span of a drug (from initial use in the clinic to the onset of resistance). The development of successful anti-virulence strategies is challenged by a redundancy of mechanisms and pathways underlying virulence expression. Optimally, the targeted virulence mechanisms are fundamental, conserved and present in multiple pathogens allowing for a broad-spectrum therapy.[24] Strategies that target pathogen specific mechanisms might only allow narrow-spectrum therapies. For those to be effectively applicable, rapid and accurate diagnostics are required in order to identify the involved pathogen(s). These diagnostics may include extended pathogen profiling (e.g. genotyping, identification of virulence factors) and may also help to improve the overall use of antibiotics in general.[29, 52]

Another challenge in the development of an anti-virulence drug may be to convince large pharmaceutical companies that have little interest in antimicrobial drug development, to support late-stage drug development of, for example, academic projects. The early stages of drug development programs are often the strength of academia and small biotechnology companies. However, the later stages largely require increased financial efforts and often demand the capacity of a large pharmaceutical company.[29]

Decreased susceptibility towards the development of antibiotic resistance and fewer undesirable effects to the host micro flora (as compared to traditional antibiotics) are considered to be the major advantages for pursuing the development of anti-virulence drugs.[5, 24] However, even if the direct selection pressure is minimized, it is unlikely that resistance against anti-virulence drugs will not develop over time. It has been demonstrated that oxidative stress (H_2O_2) selects for strains with active QS systems, e.g. mutants that are resistant to QS inhibitors.[53] Further, it can be speculated that the host immune system, which is expected to clear the infection, might exert a selection pressure itself. This might lead to the development of resistance by enhanced immune evasion (e.g. as in biofilms) or by defense mechanisms that attack cells of the immune system (e.g. as Panton-Valentine leukocidin[54]). Applying antibiotics and anti-virulence drugs in combinational therapies may allow to delay the emergence and spreading of such adapted pathogens.[29] Finally, to fully exploit anti-virulence strategies, continued research is required to improve our understanding of virulence mechanisms and potential consequences of interfering with them in the context of anti-infective therapies.[5]

2 AIMS OF THE THESIS

The overall aim of the work presented in this thesis was the discovery of novel Sortase A inhibitors and the characterization of bacterial phenotypes.

The specific objectives of the thesis were:

- Discovery and development of Sortase A inhibitors by high-throughput screening and improvement of biophysical properties by synthetic efforts (Paper I)

- Exploring the feasibility of characterizing growth condition dependent phenotypic diversity of *Staphylococcus aureus* with vibrational spectroscopy (Paper II)

- Exploring the potential of time-of-flight secondary ion mass spectrometry in conjunction with multivariate data analysis for bacterial analysis (Paper III)

- Investigating the role of the stringent response in growth phase dependent lipid modifications in *Escherichia coli* (Paper IV)

3 DISCOVERY AND DEVELOPMENT OF SORTASE A INHIBITORS (PAPER I)

The bacterial enzyme Sortase A (SrtA) has previously been identified a potential anti-virulence target. The following chapter describes the discovery and early development of inhibitors against *S. aureus* SrtA.

3.1 Sortase A

3.1.1 Biological function

The Sortase A (SrtA) enzyme is a membrane bound cysteine transpeptidase that plays a key role in the attachment of surface proteins to the cell wall in a number of Gram-positive bacteria.[55-57] These surface proteins include cell wall anchored virulence factors, such as protein A, fibronectin-binding proteins, and clumping factors which belong to the MSCRAMMs.[30, 56, 57] MSCRAMMs enable bacterial adhesion to host cells, promote infection, provide protection from the immune system, and are implicated in biofilm formation.[30] SrtA substrates are expressed as precursor proteins with a C-terminal sorting signal, consisting of a positively charged tail, a hydrophobic domain and an LPXTG motif.[56, 58] The active site of SrtA — represented by the widely conserved catalytic triad His120, Cys184, and Arg197 — recognizes the LPXTG motif of the precursor proteins. The mechanism of surface protein anchoring by SrtA is illustrated in Figure 1. The sulfhydryl group of Cys184 undergoes nucleophilic attack on the carbonyl carbon of Thr in the LPXTG motif, resulting in the cleavage of the amide bond between Thr and Gly and in turn, the formation of a thioacyl-

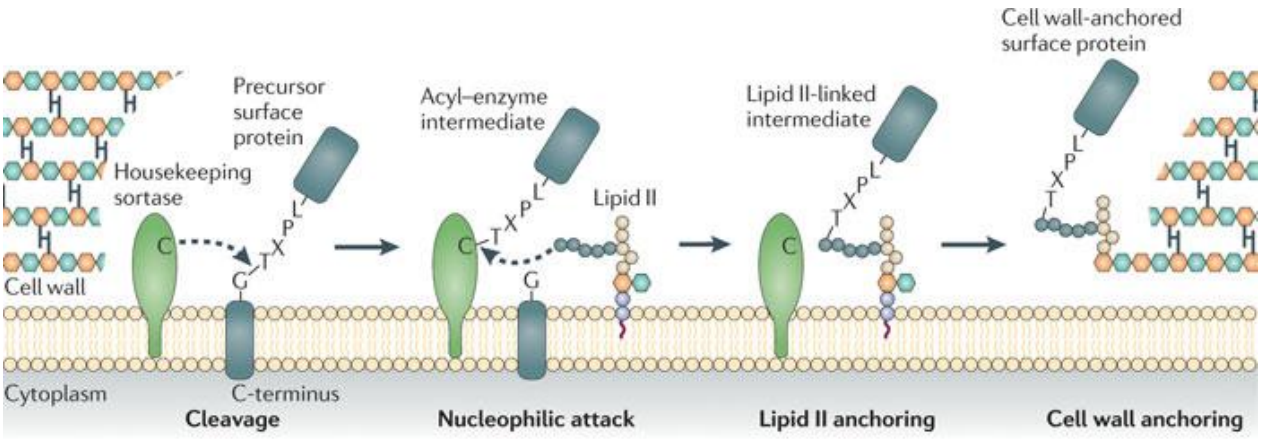

Figure 1. Illustration of the mechanism by which SrtA mediates the attachment of surface proteins to the bacterial cell wall.[57] Reprinted by permission from Macmillan Publishers Ltd: Nature Reviews Microbiology 9: 166-176, copyright (2011).

enzyme intermediate. Lipid II* is a cell wall precursor molecule that is essential for bacterial cell-wall biosynthesis.[59] The terminal amino group of the pentaglycine moiety of Lipid II attacks the carbonyl carbon of Thr within the thioacyl-enzyme intermediate. The resulting product, a protein-lipid-II precursor, is released which concludes the catalytic cycle of the SrtA transpeptidation reaction. The protein-lipid II precursor is then incorporated into the cell wall during cell wall synthesis *via* transglycosylation and transpeptidation.[57, 60]

3.1.2 Sortase A as drug target

SrtA is essential for the virulence of a number of clinically relevant pathogens, such as methicillin-resistant *S. aureus* (MRSA), and has, therefore, been recognized as a potential drug target. Gene deletion studies demonstrated the critical role SrtA plays in surface display for bacterial virulence, infection potential, and biofilm formation.[33, 61, 62] For example, *srtA* mutant *S. aureus* was incapable of causing renal abscesses and acute infection in mice, and displayed a significant reduction in mortality rates.[56, 63] Also, *srtA* mutants were more susceptible to macrophage-mediated killing.[64] Reduction of virulence and pathogenesis in animal infection models has also been reported for *srtA* mutants of other Gram-positive pathogens, such as *Listeria monocytogenes*,[65, 66] *Streptococcus pneumoniae*[67] and *Streptococcus suis*.[68] When compared to other genes of the sortase family, deletion of the *srtA* gene has been shown to have the most significant effect on pathogenesis reduction and virulence.[63] Recently, the proof of concept for the efficacy of small-molecule SrtA inhibitors as anti-infective drugs has been demonstrated.[69, 70] Importantly, *srtA* mutants are viable in rich medium, suggesting that SrtA is not required for bacterial growth which potentially reduces the selection pressure for resistance development.[33, 56, 63] The extramembranous location of the SrtA active site may be highly beneficial in facilitating the engagement of the drug, thus eliminating potential challenges that may arise due to issues associated with permeability and efflux pumps. SrtA homologs have not been identified in eukaryotic host cells and may, therefore, provide selective binding of SrtA inhibitors.[62] In addition, the conservation and the widespread use of SrtA by various pathogens may allow for the realization of a broader spectrum of drugs. In conclusion, SrtA is a promising target for therapeutic intervention by anti-virulence drugs.

3.1.3 Sortase A inhibitors

A number of compounds with SrtA inhibitory activity have been discovered by screening natural products or small molecule libraries, *via* computational strategies or rational drug design.[62, 71] A series of natural product inhibitors of SrtA is shown in Figure 2. One of the first natural products to be described as a SrtA inhibitor was *β*-sitosterol-3-*O*-glucopyranoside **1**, which was extracted from Chinese medicine plants.[72] Berberine chloride **2** was extracted from rhizomes of *Coptis chinensis* and shows slight inhibition of *S. aureus* growth (MIC 100 mg/L).[73] The SrtA inhibitors, bis(indole) alkaloid **3** and isoaaptamine **4,** were

*undecaprenyl-pyrophosphate-MurNAc(-L-Ala-D-iGln-L-Lys(NH_2-Gly_5)-D-Ala-D-Ala)-*β*1-4-GlcNAc

isolated from marine and tropical sponges, respectively.[74, 75] Additional SrtA inhibitors isolated from plant extracts include curcumin **5**,[76] rosmarinic acid **8**,[77] and chlorogenic acid **7**.[69] Chlorogenic acid **7** shows no significant growth inhibitory activity against *S. aureus* and was found to protect mice from *S. aureus*-mediated renal abscess with significantly decreased mortality.[69] Also, a number of naturally occurring flavonoids such as morin **8**,[78] quercitrin,[79] kurarinol,[80] and flavonoid glycosides[81] have been found to inhibit SrtA activity and biofilms. Wallock-Richards *et al.* rationally reduced the structural complexity of flavonoids to a common *trans*-chalcone **9** scaffold. They demonstrated that *trans*-chalcone **9** inhibited SrtA and *Streptococcus mutans* biofilm formation *in vitro* by irreversible binding to SrtA Cys184.[82] Further, dihydro-*β*-carboline **10** is a SrtA inhibitor derived from marine sponge natural products with no inhibitory effect on bacterial growth.[83]

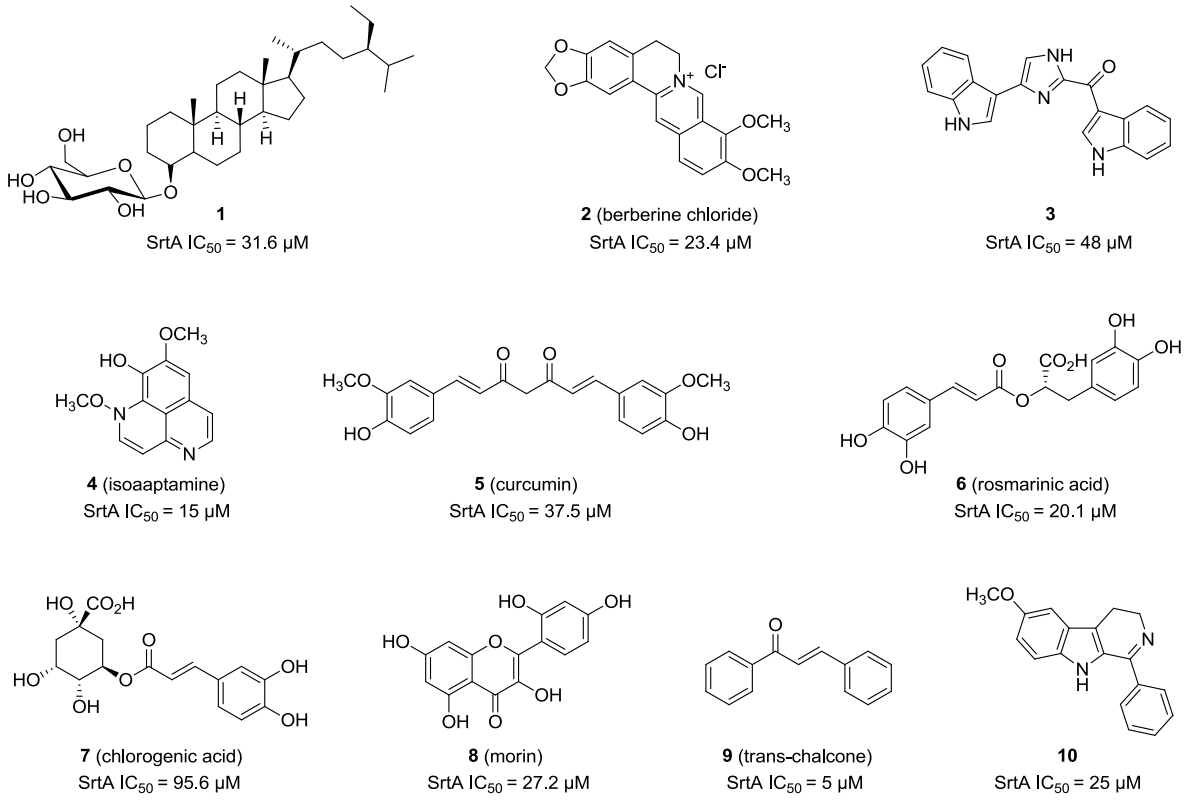

Figure 2. Natural product inhibitors of SrtA.

Additional SrtA inhibitors were found by high-throughput screening (HTS) or *in silico* screening efforts from small-molecule libraries and are shown in Figure 3. The diarylacrylonitrile **11** proved to be the most active compound in an optimization series of a lead compound discovered by HTS. Diarylacrylonitrile **11** displayed reversible binding to SrtA and decreased renal infections in mice models infected with *S. aureus* Newman. While mortality rates were reduced, compound **11** exhibited undesirable toxic side effects.[84] Aryl(*β*-amino)ethyl ketone (AAEK) **12** displays irreversible inhibition of SrtA through the formation of covalent bonds to the Cys184 within the active site.[85] Suree *et al.* discovered rhodanine **13**, pyridazinone **14**, and pyrazolethione **15** as novel SrtA inhibitors resulting from optimization

of HTS hits.[86] Zhulenkovs and co-workers reported a series of benzisothiazolinone-based SrtA inhibitors such as compound **16** that displayed IC_{50} values ranging from 3.8–12.8 μM. Most of the benzisothiazolinones inhibited NIH 3T3 mice fibroblast cells (IC_{50} 1.3–263 μM) and bacterial growth *in vitro*.[87] Rebollo *et al.* recently described a macrocyclic peptide that inhibits SrtA reversibly with an IC_{50} value of 167 μM.[88] More recently, phenylhydrazinylidene derivatives (such as compound **17**) have been reported as modest SrtA inhibitors that inhibited biofilm formation but not bacterial growth *in vitro*.[89] Zhang *et al.* discovered the 3,6-disubstituted triazolothiadiazole **18** through *in silico* screening and subsequent optimization. Compound **18** was found to inhibit SrtA without affecting bacterial growth and protected mice from lethal *S. aureus* bacteremia.[70] Several of the shown SrtA inhibitors may result in covalent modification of the active site, despite some being reversible binders.

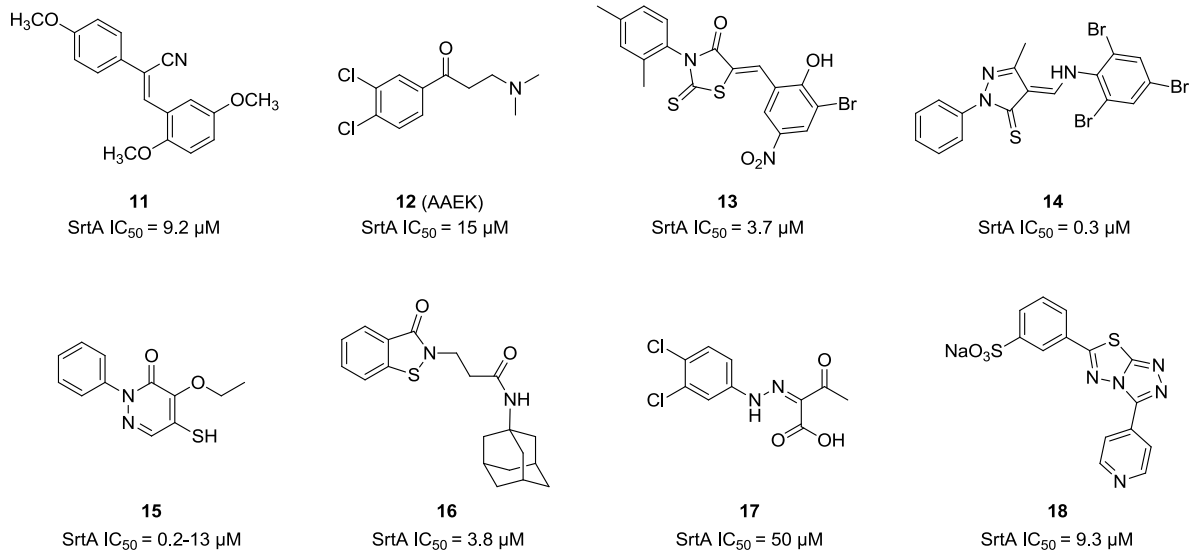

Figure 3. Inhibitors of SrtA discovered by screening of small-molecule libraries.

Recent advances in this field have seen the development of SrtA inhibitors with IC_{50} values in the low micromolar range. However, despite these recent efforts, many of the SrtA inhibitors have insufficient potency, undesirable structural features, selectivity issues, and require further optimization in order to be therapeutically useful.

3.2 Biophysical Evaluation Methods

3.2.1 FRET based functional SrtA assay

Functional assays, based on fluorescence resonance energy transfer (FRET), have previously been successfully applied to screen for SrtA inhibitors.[71] FRET is a non-radiative energy-transfer process that occurs between a donor and an acceptor molecule in close proximity (typically distance $r < 10$ nm).[90] The energy is transferred through long-range dipole–dipole interactions and is thus highly distance-dependent (inversely proportional to

r^6).[91] Furthermore, FRET depends on the overlap of the absorption and emission spectra of the acceptor and the donor, respectively, and on their transition dipole orientations. This distance-sensitivity of FRET can be exploited to investigate molecular interactions.

3.2.2 NMR (CPMG) protein binding assay

One-dimensional ^{1}H Carr-Purcell-Meiboom-Gill (CPMG) relaxation dispersion NMR experiments were performed for ligand-detected protein binding.[92] The CPMG relaxation dispersion exploits the differential T2 relaxation properties of a ligand in free or protein-bound state to indicate protein binding. When a ligand binds to a protein, its rotational correlation time assumes that of the protein (increases). This leads to shorter relaxation times and results thereby in line-broadening. In a CPMG relaxation dispersion experiment a series spin-echo pulse elements are applied to refocus the spreading spins (T2 relaxation) precessing in the transverse plane. The spin-echo element (τ-$180_{x,y}$-τ) contains a 180° radio-frequency pulse and two relaxation delays τ (~0.25-25 ms). The spins can be refocused if their average chemical shift during the two τ periods are identical. However, if the chemical shifts during the τ periods are different, for example when a ligand translates from free and protein-bound state, the spins do not return symmetrically and will, therefore, not refocus. NMR spectra of the ligand are recorded in both the absence and presence of the protein (usually, with a ligand-to-protein ratio of 10:1). A binding interaction will result in a decrease in signal intensity, provided the exchange between the free and bound state is in the intermediate-fast regime. Ligand binding to the protein can be detected over the μM-mM affinity range. Ligands with high affinity have low dissociation rates, and exchange therefore slowly. This may result in false negatives as the signal decreases only slightly (depending on the ligand-to-protein ratio). The reversibility of binding can be assessed through competitive binding experiments, whereby a known binder is added. Subsequent recovery of the signal may indicate reversible binding.[93, 94]

3.2.3 Surface plasmon resonance (SPR) spectroscopy

SPR spectroscopy was used for studying ligand-SrtA binding interactions to quantitate binding affinities and kinetics. SrtA protein is immobilized onto a sensor chip surface (functionalized gold film on glass support) within a flow cell. Ligand molecules in solution are passed over the chip surface allowing the ligand to interact with the bound SrtA. Binding interactions with ligand molecules change the refractive index of the medium in near the chip surface which can be monitored in real time. This allows to accurately measure the binding affinity through association and dissociation kinetics of the interaction.

SPR spectroscopy exploits the phenomenon of surface plasmon generation. Polarized light is directed through a prism, reflects off the backside of the gold film and subsequently passes into a detector. At a certain incidence angle (resonance angle), the light is absorbed by the electrons in the gold film causing them to resonate (surface plasmons). This absorption leads to a decrease in intensity of the reflected light and gives rise to minimum in the SPR

reflection intensity curve. The SPR angle is dependent on the refractive index of the medium close to the gold surface and changes, for example, during binding interactions.[95, 96]

3.3 Discovery and Development of Sortase A inhibitors (Paper I)

[Unpublished data has been removed in this e-publication.]

4 TOWARDS A GLOBAL ESTIMATE OF BACTERIAL PHENOTYPIC DIVERSITY (PAPER II)

As a result of adaptation to the environment, bacteria display phenotypes with variable virulence properties and susceptibilities to antimicrobials. A global estimate of bacterial phenotypic diversity based on principal components analysis (PCA) and Fourier transform infrared (FTIR) fingerprinting may allow for the identification of a subset of growth conditions under which newly developed antimicrobials could be evaluated for their efficacy against different phenotypes. In the following chapter, the feasibility of utilizing FTIR spectroscopy for the characterization of bacterial phenotypic diversity of *S. aureus* grown under variable sets of environmental conditions was explored.

4.1 FTIR Spectroscopy as Tool for Rapid Bacterial Phenotyping

Vibrational spectroscopy techniques have previously been successfully applied for the characterization, discrimination and identification of microorganisms.[97] In particular, transmission FTIR spectroscopy was found to be capable of bacterial discrimination on strain and sub-strain level.[98, 99] Additionally, Fourier transform infrared spectroscopy-attenuated total reflectance (FTIR-ATR) of fatty acid methyl esters (FAMEs) has been successfully employed to distinguish bacteria on a phenotypic level.[100] In contrast to analysis methods that investigate a small sub-set of the sample chemistry, FTIR spectroscopy provides insight into the total composition of bacterial cells. FTIR spectra can be measured on intact bacterial cells with minimal sample preparation. As a result, the spectra are composed of the superposition of contributions from the cells' biomolecules. Interpretation of the spectra can be guided by five spectral regions that are important for bacterial characterization (Figure 4 and Table 1). In conclusion, FTIR spectroscopy offers quick and sensitive analysis with, however, limited structural information of the sample chemistry.

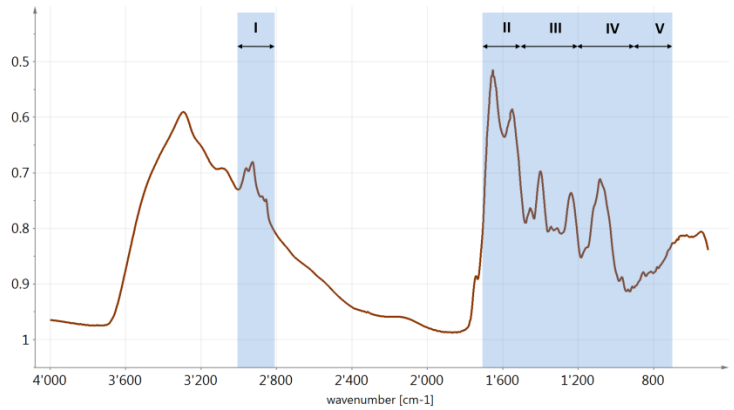

Figure 4. Spectral regions in the FTIR spectrum of *S. aureus* relevant for bacterial characterization. Annotations are listed in Table 1.[101]

Table 1. IR regions with characteristic information for bacterial analysis, as illustrated in Figure 4.[101]

No.	Information	Spectral region [cm^{-1}]
I	Fatty acids CH-stretching	3000-2800
II	Amide I and amide II bands of proteins and peptides	1700-1500
III	Fatty acids, proteins, phosphates containing species	1500-1200
IV	Polysaccharides CO-stretching	1200-900
V	Unique bacteria specific absorbances	900-700

4.2 Design of Experiments

Design of Experiments (DoE) is an efficient procedure for the strategic planning of experiments involving multiple variables (factors). It aims to maximize the information gained from a minimal number of experiments by simultaneously changing variables and observing the resulting effects on the responses. Thereby, defining relevant experimental factors at meaningful levels and appropriate responses is critical for the informative value of the resulting data. Mathematical models are used to describe the relationships between factors and responses, as well as interactions between the factors (synergy, antagonism). A full factorial design comprises experiments of all combinations of k factors at two levels. This results in 2^k experiments that are usually supplemented with a triplicate center point to recognize non-linear relationships and to determine confidence intervals. Such designs are balanced and orthogonal, which allows for the generation of unbiased estimates. The models allow for the recognition of optimal factors settings and can therefore be used in the optimization and the testing of robustness of methods and products. Experimental design is an efficient way to systematically examine multi-factor systems in order to obtain valid and objective conclusions.[102]

4.3 Multivariate Data Analysis (MVA)

4.3.1 Principal components analysis

Principal components analysis (PCA) is a powerful statistical technique for extracting meaningful information from data with multiple variables. PCA is a mathematical procedure that reduces the dimensionality of complex multivariate data while retaining most of the variation within the data set. Dimensionality reduction is achieved by identifying directions with the largest variation in a data set, the so called principal components (PCs). The first principal component is the direction with the largest variation in the data set. Further components are directions with the largest variation that are orthogonal to previous components. Each observation obtains a score value for each component, which are co-ordinate values for the new projection. The data is then represented using scores plots, which

allows for the appreciation of an entire set of data with fewer dimensions. The data can then be visually examined to interpret the data structure and to identify patterns and relationships. The information on how the variables contribute to the scores may be drawn from by the PCs' loadings. The quality of input data is critical as PCA only changes their projection for enhanced interpretability. Variation caused by systematic experimental artifacts may result in dominant PCs. Therefore, knowledge of the experimental procedure and understanding of the methods used to create the data is of advantage for drawing appropriate conclusions.

Data preprocessing

Data often have to be pretreated in order to obtain a useful PCA model. This usually includes mean-centering and scaling the data set. Additional preprocessing procedures include transformations, corrections and compressions. Mean-centering subtracts the average of each variable from the data, both simplifying the PCA algorithm and improving the interpretability of the model as a result.[103] In this work, all data were mean-centered prior to PCA, either without or in combination with scaling methods. Since PCA weights are based on variation, large variables having large variances would have a higher contribution in the PCA model. Therefore, scaling can be used to normalize the often large numerical ranges and thereby largely different variances of variables. Unit variance (UV) scaling is the most commonly used scaling method. In UV scaling, the data are divided by the standard deviation of each variable. As a result, all variables obtain an equal chance of influencing the model. Alternatively, Pareto scaling divides each variable by the square root of the standard deviation, representing an intermediate scaling method between unit variance scaling and no scaling.

Further preprocessing methods can be applied to e.g. FTIR spectral data to remove physical effects that are caused by light scattering, random noise, small film thickness variations, and baseline drifts. Methods used for spectral preprocessing include normalization, orthogonal signal correction (OSC), standard normal variate (SNV) transformation, multiplicative scatter correction (MSC), Savitzky–Golay (SG) smoothing and the application of derivatives.[15, 99, 100, 104, 105] In MSC, each observation is normalized by regressing it against the average spectrum. Data treated with SNV transformation are normalized by subtracting the mean and dividing by the standard deviation. The application of derivatives may be useful for normalizing baseline offset. SG smoothing is often applied in combination with derivatives in efforts to mitigate adverse effects of derivatives on noise. The degree of SG smoothing is adjusted by varying the range of the moving average.[103]

Cross validation

Cross validation (CV) is a model validation technique used to assess the predictive ability of a model. During CV, the data set is divided randomly into equally sized parts (e.g. seven equal blocks). Each part is then once excluded from the model building and used as a test set. The values predicted for the test sets are finally compared with their actual values to then calculate the predictability value Q^2. CV is a useful measure to estimate the numbers of significant principal components and to limit problems like overfitting.[106]

4.3.2 Orthogonal Partial Least Squares projections to latent structures (OPLS)

OPLS is another multivariate statistical method based on dimensionality reduction. In contrast to PCA, which identifies maximum variance in a data set (X-matrix), the OPLS discriminant analysis algorithm maximizes the separation of classes and is based on linear regression. The OPLS projection is guided by supplied class information (Y-variables) and is, therefore, a supervised method, whereas PCA is unsupervised. The variability in the X-matrix is divided into systemic and residual variability. The systemic variability is further divided into a predictive part that is correlated to Y and an orthogonal part that is uncorrelated to Y. The objectives are to identify which X-variables in the data set drive class separation.[107]

4.3.3 Multiple linear regression

Multiple linear regression (MLR) is a statistical technique for modelling linear relationships between independent explanatory variables and a dependent response variable. It is therefore well suited for analyzing the relationship between the orthogonal factors of a factorial design. Linear curve fitting is achieved by minimizing the sum of squared deviations. Thereby, the independent variables are fit separately. MLR aims to predict the degree of influence the independent factors have on the response variable.

4.4 Investigation of Bacterial Phenotypic Diversity (Paper II)

In order to determine whether the phenotypic diversity of *S. aureus* could be characterized using FTIR spectroscopy, appropriate methods needed to be developed. Initial efforts included the establishment of a suitable instrumental setup and protocol for efficient sample preparation so that reproducible results could be realized. Cultures of *S. aureus* were then grown in various conditions according to an experimental design and the spectral data obtained from their FTIR analysis were investigated by PCA.

4.4.1 Selection of the instrumental setup

Transmission FTIR spectroscopy was selected for the analyses of this study after comparison to FTIR-ATR spectroscopy and Raman spectroscopy. The apparent advantages of transmission FTIR spectroscopy included its high sensitivity (required for the analysis of biofilms) reproducibility, and the potential for rapid throughput. A quick sample throughput was realized by acquisition settings and the implementation of a custom made xy-stage (*Appendix 8.4*). A comparison of optical substrates including zinc selenide (ZnSe), silicon waver, and polyethylene resulted in the selection of ZnSe due to reproducible quality of the optical windows. The optical quality was further improved by the application of a monocrystalline ZnSe well plate (*Appendix 8.5*). Reproducibility of the combined instrumental setup, including the FTIR instrument, xy-stage, and ZnSe well plate, was validated by close clustering of spectra from repeated recordings on PCA scores plots (Figure 6).

4.4.2 Development of bacterial sample preparation

In order to preserve the authenticity of bacterial samples, sample preparation was kept to a minimum by simple washings of the cells. As a consequence, the bacteria remained viable. As such, the time-span from harvesting to analysis was kept short to prevent the occurrence of metabolic changes when removed from treatment conditions.[14] Harvested cells were washed three times with pure water to remove confounding contributions from growth medium. The various cultivation conditions led to differential growth rates and resulted thus in unequal cell densities of cultures (OD_{590nm} 0.44–1.22). By taking into consideration the various optical densities, sample concentrations could be adjusted to achieve equivalent biofilm thicknesses when applied onto the ZnSe well plate. Potential small film thickness variations could be treated by spectral filters. The even application of samples was crucial for the reproducibility of results. Due to the low wettability properties of ZnSe, aqueous samples are challenging to apply evenly. A small amount of detergent (0.0005% Tween20) in the sample dilution was included to allow for an even application. Further, applying small sample volumes (5 µL) kept drying durations (20 min, 40 °C) and sample preparation time to a minimum.

4.4.3 Experimental design of cultivation conditions

Factors chosen for the full factorial design were pH, temperature and salinity with ranges selected to include potential variation in conditions observed in wound sites.[108] A graphical illustration of the experimental design is shown in Figure 5 with treatment conditions listed in Table 2. Implementation of this design aimed primarily on an even and well balanced sampling of conditions for analysis by PCA, rather than the commonly used MLR evaluation of factors.

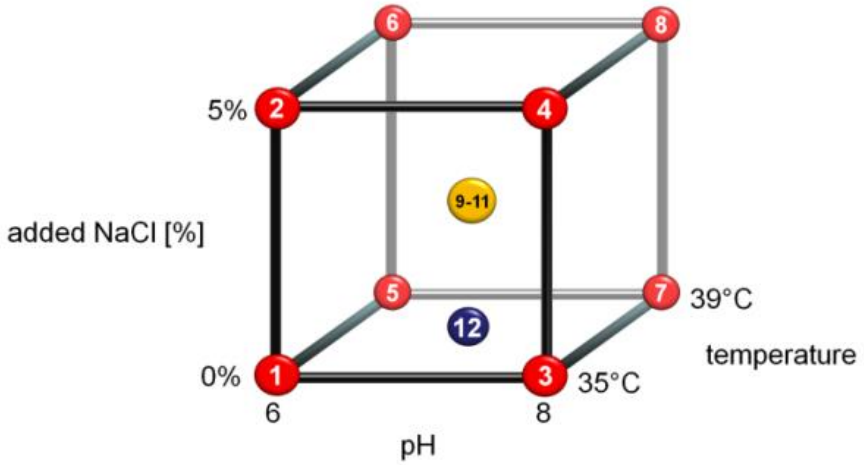

Figure 5. Schematic representation of the experimental design with limit conditions for environmental factors (red) under which cultures of *S. aureus* were grown. Additionally, the standard cultivation condition (blue) and the center-point condition (orange) were included. The numbering corresponds to treatment groups in Table 2 and Figure 7.

Table 2. Treatment groups and their combinations of cultivation conditions used in the full factorial design.

Treatment Group	NaCl conc [% w/w]	pH Value	Temperature [°C]	
1	0	6	35	factorial limit conditions
2	5	6	35	
3	0	8	35	
4	5	8	35	
5	0	6	39	
6	5	6	39	
7	0	8	39	
8	5	8	39	
9	2.5	7	37	center point (n = 3)
10	2.5	7	37	
11	2.5	7	37	
12	0	7	37	standard cultivation condition

4.4.4 Preparation of FTIR spectral data for MVA

FTIR spectra were obtained from all cultures grown according to the experimental design (Figure 6A). The raw spectra were visually inspected to carefully select spectral regions for PCA. IR regions with small within-group variation, as highlighted in Figure 6A, did not appear to contain information important for group differentiation. Some of these variations are likely to arise from water contributions (absorbing at 4000 to 3300 cm^{-1} and 2200 to 1200 cm^{-1})[105], however, no correlations to the order of sample preparation were identified. SNV transformation emphasized the strong similarity between the spectra of the different groups, as shown in Figure 6B. There, regions with observed differences between spectra of the treatment groups are highlighted. Several of those have been reported to be useful for bacterial characterization[109] and the discrimination of a mutation induced SCV phenotype.[98] Savitzky-Golay (SG) smoothing of spectral noise reduced small variations and was done to avoid the unfavorable effect of noise during first derivation.[98] A SG-smoothing average over 45 points appeared optimal, regarding PCA clustering, for data recorded with a resolution of 4 cm^{-1} and 8 averaged scans (Figure 6C). The data were UV scaled (and centered) as a last step of data pretreatment prior to PCA. As differences between the treatment groups were expected to be small, it appeared appropriate to scale all absorbance values to unit variance. The combined preprocessing methods included following steps:

1. SNV transformation
2. SG-smoothing (quadratic order, 45 points of smoothing)
3. First derivative (quadratic order, 15 points of smoothing)
4. Restriction of spectral regions (3600-2450 cm^{-1} and 2200-700 cm^{-1})
5. UV scaling, centering

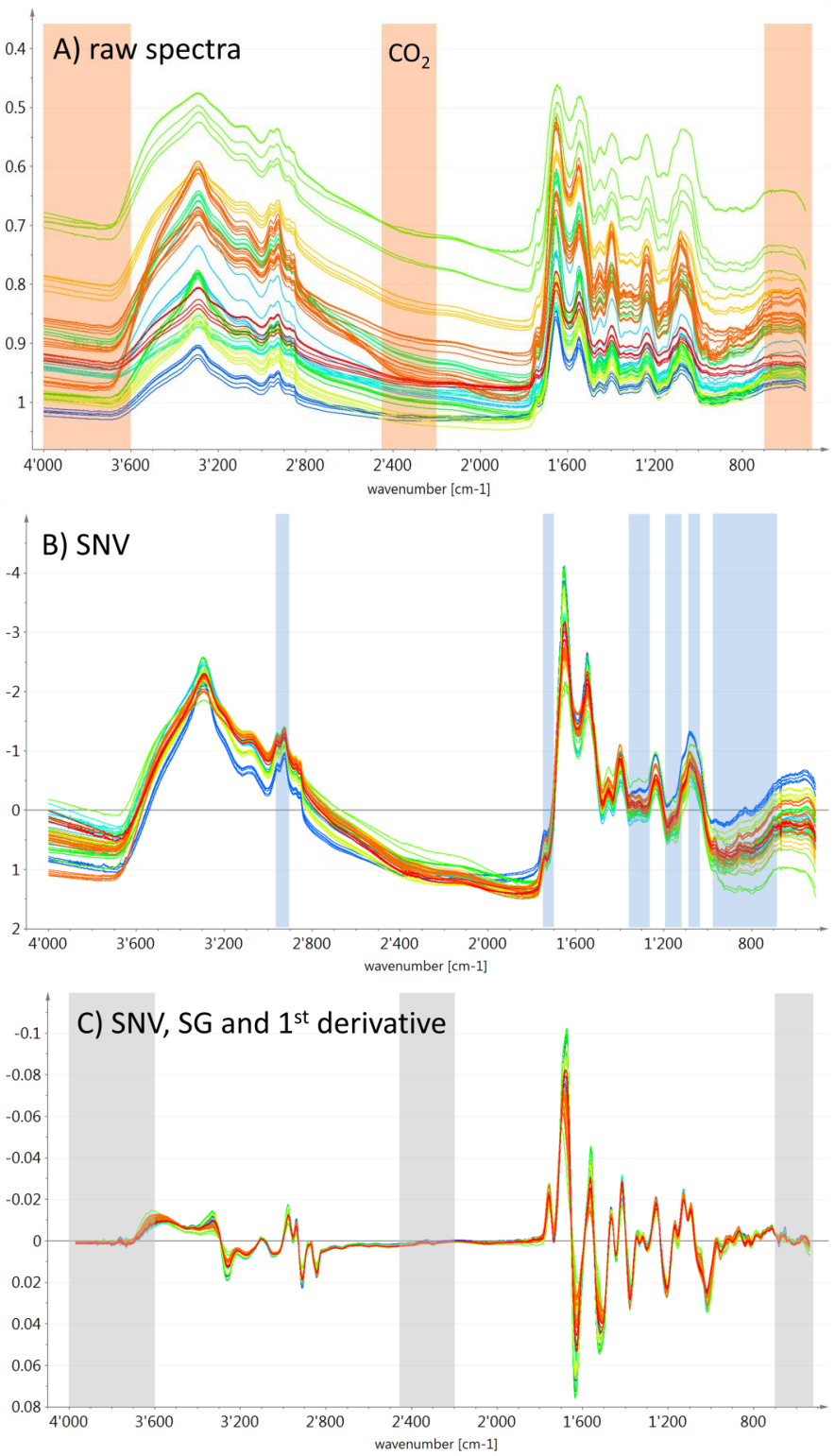

Figure 6. Preprocessing of FTIR spectra obtained from all bacterial treatment groups. A) raw spectra, regions of within-group variations are marked (4000–3600 cm^{-1}, 2450–2200 cm^{-1}, <700 cm^{-1}), the spectral region 2450 to 2200 cm^{-1} may include variations in characteristic signals from CO_2; B) spectra after SNV transformation, spectral differences between treatment groups are marked (2970-2840 cm^{-1}, 1760-1710 cm^{-1}, 1370-1270 cm^{-1}, 1200-1130 cm^{-1}, 1025-1100 cm^{-1}, and 990-700 cm^{-1}); C) Chained filters: SNV transformation, SG-smoothing and first derivative, grey marked regions were excluded from PCA.

4.4.5 MVA and interpretation

The application of the preprocessing procedure for the FTIR spectral data previously described in *Section 4.4.4* achieved distinct clustering in PCA (Figure 7). All treatment groups were separated using the first three most significant principal components accounting for 73% of the variability in the data set. A total of seven components were found to be significant ($R^2X(cum) = 0.94$) as assessed by cross validation ($Q^2X(cum) = 0.91$; see *Appendix 8.6* for further model details). Sharp clustering indicates useful reproducibility including replication of the instrumental setup. The center-point groups 9, 10 and 11 were included for assessing the reproducibility. The sterile broth for group 9, however, was left unfiltered in contrast to the broths of all other groups. This deviation may have contributed to separate clustering of group 9 on the scores plot PC1 vs PC3 (Figure 7B). The unfiltered broth may have contained gel like matrix material. In conclusion, it appears that broth filtration is important for the reproducibility. Further, cluster variation of treatment group 6 (5% NaCl, pH 6, 39 °C) may be explained by differences in the applied sample films. The bacteria in the planktonic culture of group 6 were observed to aggregate, which could have led to variable film representations. Furthermore, this observation might suggest an *in vivo* biofilm forming phenotype.

The observation of clear cluster separation led to the conclusion that each combination of treatment conditions yielded cultures with a unique and characteristic FTIR profile. Each of those profiles may indicate bacterial phenotypic adaptations to cultivation conditions. Similar observations were made by Crompton *et al.* 2014 where treatment conditions led to alterations in GC/MS lipid profiles of *S. lugdunensis*.[108]

The largest variations in the data set appear to arise from differences in salinity and pH - as judged by clustering on scores plot PC1 vs PC2 (Figure 7A). Temperature variations in the applied range seemed to have affected the cultures only to a lesser extent as a slight trend for the effect of temperature could be assumed along PC6 (*Appendix 8.6*). These trends were further investigated in an OPLS model using salinity, pH, temperature, and OD as Y-variables. Predictive components 1 to 3 separated the groups based on salinity, pH, and temperature differences in their treatment, respectively. No clustering for OD was obtained in any combination of components (see *Appendix 8.7* for model details and scores plots). These results suggest that salinity contributes most to the differences in the treatment groups, closely followed by pH. It also confirmed that the temperature variations affected the cultures only to a small extent.

In conclusion, these results suggest that investigating *S. aureus* phenotypic diversity by multivariate data analysis of FTIR spectra obtained from cultures grown under various conditions is feasible. Future investigations could include additional conditions to establish a global estimate of phenotypic diversity by an analogous approach as that for the ChemGPS (Chemical Global Property Screen) initiative.[110] The strategy initially aimed to assess growth

inhibitory properties of bacteriostatic and bactericidal antibiotics on potential phenotypes. However, for exploring the efficacy of anti-virulence agents with this strategy, alternative assays would have to be employed. For inhibitors of SrtA, for example, an adherence assay under various environmental conditions could be implemented.

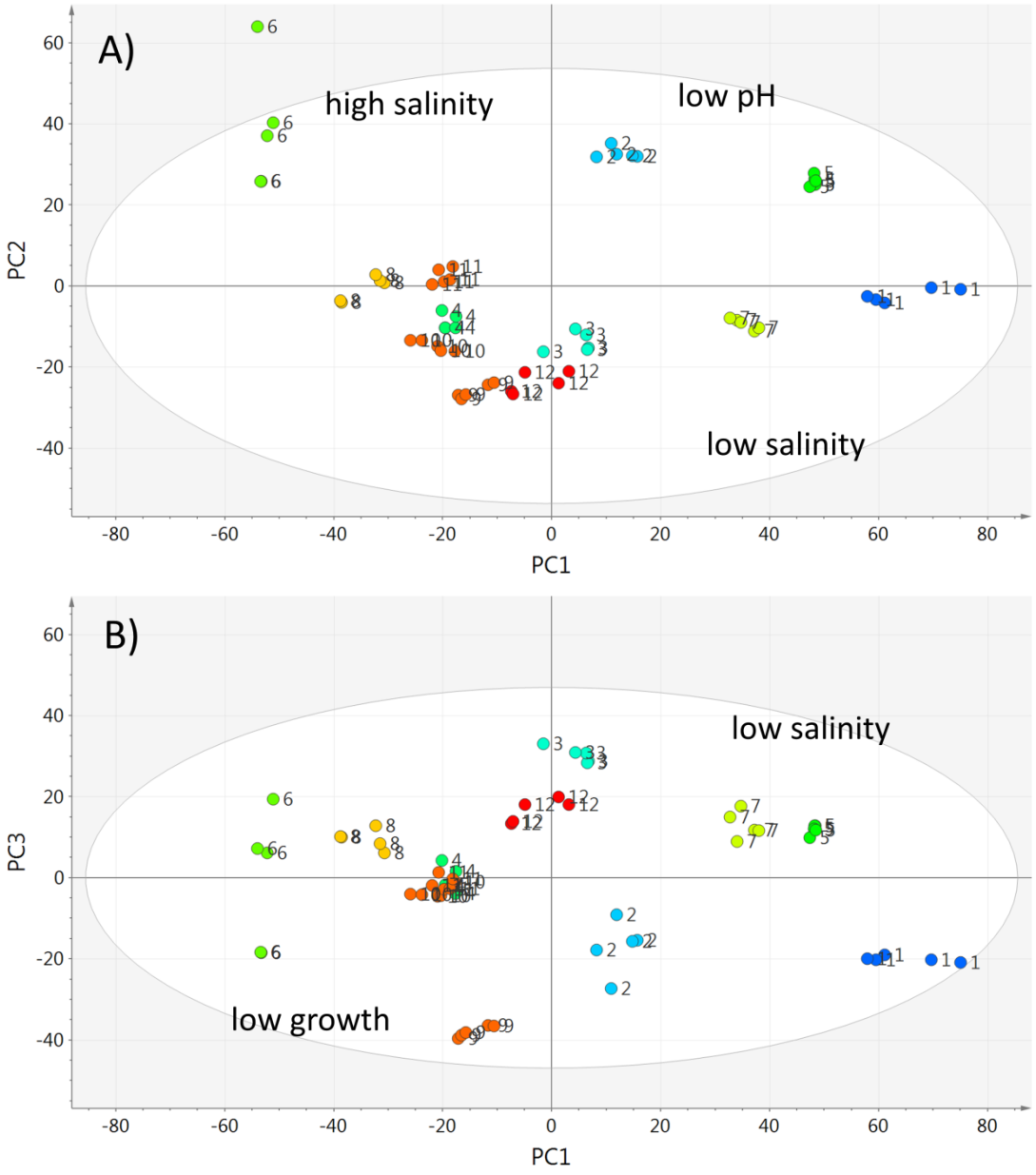

Figure 7. PCA scores of FTIR spectral data displaying full separation of all treatment groups (n = 10, 5 measurements each) using 3 principal components ($R^2X(cum)$ = 73%). UV scaled, data pretreatment as described in *Section 4.4.4*. Colorations indicate treatment group, numbering refers to treatments in Table 2, and annotations suggest trends. Ellipse: 95% confidence interval.

4.4.6 Impact of factors on the optical density of cultures

The various conditions of the experimental design affected growth and final optical density of the *S. aureus* cultures (OD_{590nm} 0.44-1.22). MLR was used to examine treatment factor relationships and their impact on the OD as response variable. The obtained MLR model was significant ($R^2 = 0.92$, $Q^2 = 0.77$), included all factors and the synergistic estimate for NaCl*pH. Contour plots as presented in Figure 8 display the condition dependence of the OD. Increase in temperature resulted in elevated bacterial growth independent of pH and salinity. Low pH and high salinity decreased growth whereas cultures in high pH generally yielded higher ODs.

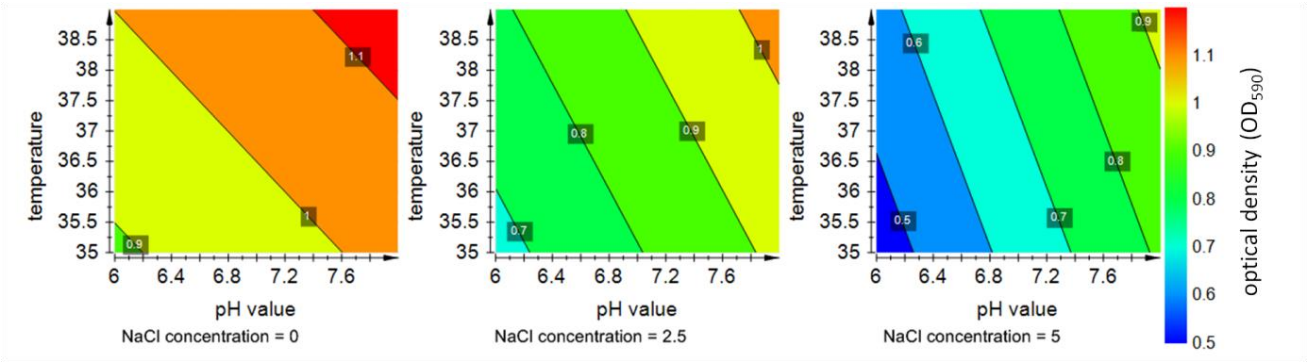

Figure 8. MLR contour plots displaying variations in the optical density of *S. aureus* cultures as a result of different cultivation conditions. Generally, an increased temperature and pH led to a higher OD, whereas high salinity and low pH resulted in a decrease of the final OD.

4.5 Summary of Paper II

FTIR spectroscopy was selected for the analyses in this study due to its sensitivity, rapidity and potential to analyze live cells. In summary, cultures of *S. aureus* were grown under various environmental conditions according an experimental design. Transmission FTIR spectra obtained from each treatment group were preprocessed prior to PCA. The applied data preprocessing procedure included SNV transformation, SG smoothing and first derivative, and restriction of spectral regions. In a PCA model with UV scaling, all treatment groups were fully separated using the first three most significant principal components ($R^2X(cum) = 0.73$). Salinity and pH appeared to contribute most to the differences in the treatment groups, whereas temperature variations had little effect. These observation are sensitive to the applied ranges of conditions. In conclusion, transmission FTIR spectroscopy in conjunction with experimental design, and multivariate analysis, presents a powerful tool for the investigation of the phenotypic diversity of *S. aureus*. The limited interpretability of resulting FTIR spectra could potentially be complemented by additional analysis methods that probe the chemistry specifically.

5 MASS SPECTROMETRIC SURFACE ANALYSIS FOR BACTERIAL CHARACTERIZATION (PAPER III AND IV)

Time-of-flight secondary ion mass spectrometry (ToF-SIMS) was used to further characterize bacterial phenotypes. An initial feasibility study included the analysis and multivariate differentiation of a set of four bacterial strains. In a subsequent study, changes in membrane lipids as a result of adaptation to starvation stress in *E. coli* were investigated.

5.1 ToF-SIMS

ToF-SIMS is a highly sensitive surface analysis technique that acquires elemental and molecular information through direct analysis of sample surfaces. It allows for the interrogation of inorganic, organic and biological surfaces without the requirement for derivatization or labeling. By bombarding the sample surface with a high energy primary ion beam (usually 10s of keV), analyte species are ejected as secondary ions and subsequently analyzed by ToF mass spectrometry. By rastering a fine-focused primary ion beam over a sample surface, a mass spectrometric image can be obtained where each pixel represents a mass spectrum. These high resolution chemical images can be used to visualize the spatial distribution of the chemical constituents in the sample. The analysis can be extended into three dimensions by etching the sample surface layerwise to create a 3D chemical image.[111]

Due to the small ionization probability, the secondary ion yield is usually very low and limits the analysis at submicrometer resolution. Highest yields are obtained from easily ionizable molecules such as lipids and small metabolites. The properties of the primary ion beam affect the extent of analyte fragmentation and the potential of spatial resolution. Atomic ion sources (Cs^+, O_2^+) allow for narrow focus (<50 nm) and yield a high fragmentation with little molecular information. The application of cluster (Au_3^+, Bi_3^+) and polyatomic (SF_5^+, C_{60}^+) ion beams have greatly improved the yield of higher mass intact molecular type species.[112-115]

Recent advances in the field include the application of gas cluster ion beams (GCIBs) which bring considerable benefits especially for the analysis of biological samples.[116, 117] GCIB technology facilitates the generation of higher mass species (m/z up to a few thousand) and closes the mass range gap between SIMS and matrix-assisted laser desorption ionization (MALDI) mass spectrometry.[118] Mass spectrometry imaging with ToF-SIMS has become increasingly popular for studying complex biological materials such as cells and tissues.[118-120] To date, ToF-SIMS has been successfully applied for the analysis of bacterial isolates from urinary tract infections,[121] bacterial biofilms,[122] investigations of *Streptomyces coelicolor* populations[123] and for the discrimination of Bacillus strains.[124] Furthermore, ToF-SIMS coupled with tandem MS has been investigated for metabolomics.[125]

5.1.1 J105 3D Chemical Imager

The J105 ToF-SIMS instrument (Figure 9) implements a new SIMS design and is still subject to continuous development. In the J105 instrument, the primary ion beam is operated in a quasi-continuous mode, which generates a secondary ion stream that is led into a buncher where it is focused into packets of ions. These are then accelerated into a quadratic field reflectron mass analyzer and subsequently detected. Ion bunching enables the quasi-continuous operation of the primary ion source and decouples the mass spectrometry from the sputtering process. This eliminates the need for mass calibration for every spectrum and allows the analysis of topographically challenging samples with high mass accuracy. Thereby, the mass resolution is independent of the spatial resolution which, in principle, enables simultaneous acquisition with both resolutions at their best. Furthermore, compared to conventional pulsed ion beam SIMS systems, the J105 ToF-SIMS design greatly reduces spectral and image acquisition times. The acceleration in the buncher results in an increased energy spread (6 keV) of the secondary ions, which necessitates the application of a harmonic field ToF reflectron. In there, the ions are separated according to the mass and charge and not their energy. The bunching quality is critical as the time focus of secondary ions at the entrance of the reflectron affects the mass resolution.[126]

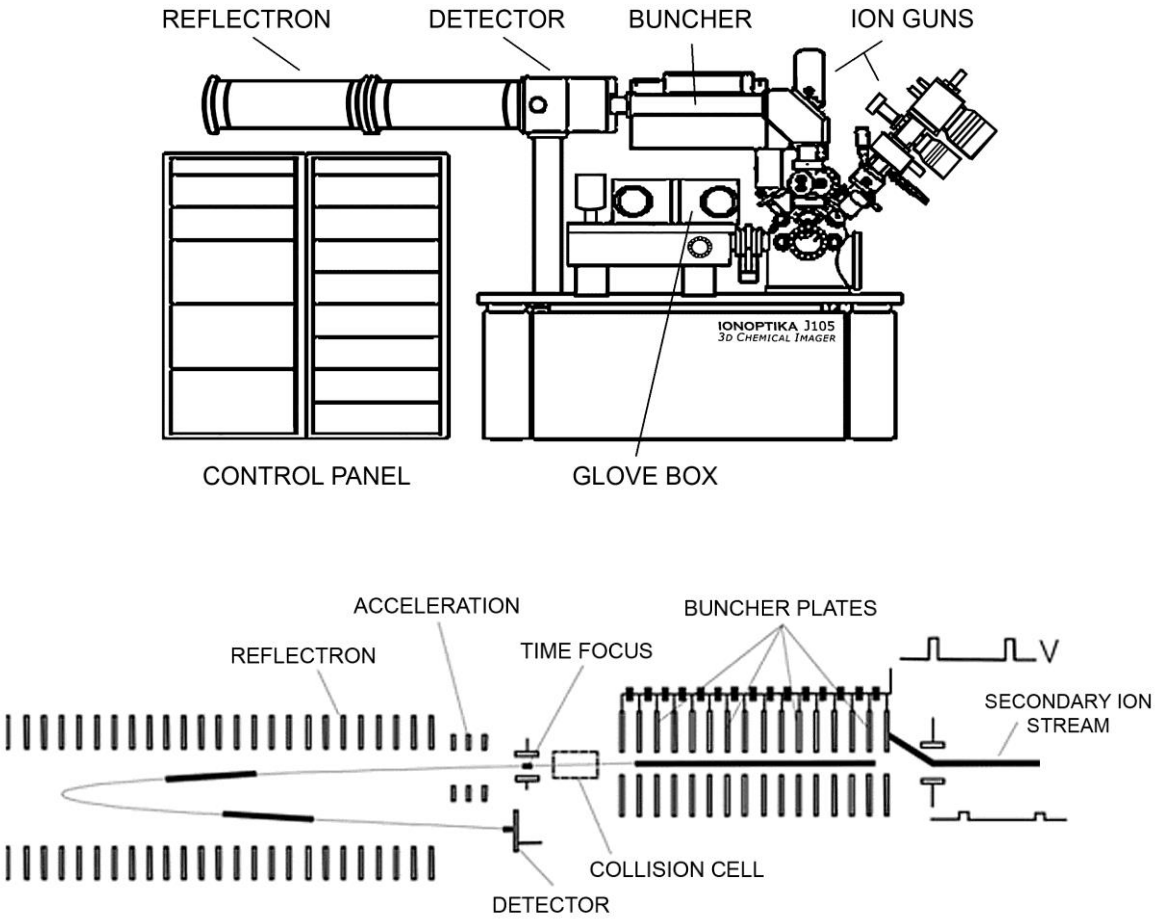

Figure 9. Schematics of the J105–3D Chemical Imager. The secondary ion stream is bunched into a focus before entering the harmonic field reflectron ToF analyzer.[126]

The J105 instrument is capable of tandem MS, which is performed in a field free region right after the buncher by collision induced dissociation (CID) of the secondary ions with Ar gas. Fragment ions and their precursor continue to move with the same velocity and are selected using a timed ion gate subsequent to a short ToF region.[126]

5.2 Bacterial differentiation using ToF-SIMS and MVA (Paper III)

In an initial study, the potential of using ToF-SIMS in conjunction with MVA for bacterial analysis was explored. Primary aims included the optimization of data preprocessing for optimal cluster separation in PCA to study small chemical differences that would ultimately allow for phenotypic characterization. In order to represent three fineness-levels of differences, a set of four bacterial types and strains was used including *P. aeruginosa*, *E. coli*, and two strains of *S. aureus*. The largest difference therein was expected to be between the Gram-negative and Gram-positive bacteria. The cell envelopes of the Gram-negatives themselves may differ on another level and the strains of *S. aureus* may show only subtle differences. With this approach at least three levels of differences were expected to be represented in subsequent multivariate modelling. Bacterial samples from each of the four strains were obtained after simple washing of cells from an overnight culture in rich medium. The samples were applied onto silicon waver and dried prior to ToF-SIMS analysis using a C_{60}^+ primary ion beam. Resulting mass spectrometric data were investigated with exploratory PCA.

5.2.1 Exploratory PCA of ToF-SIMS data

Data preprocessing and scaling methods, as described in *Section 4.3*, were applied to optimize clustering in PCA. In addition, data binning was used to mitigate possible peak-shift errors that may have arisen from temperature variations during data acquisition. Statistical analysis methods like PCA are sensitive to variation of corresponding signals between observations, known as the correspondence problem.[127] Data binned over 10 data points achieved best cluster separation, for the present data set, compared to no binning, or binning over 5 or 20 data points. In later studies, data binning was avoided to due to potential binning-related artifacts.

Initially, PCA was used to individually examine data from the positive and negative ion modes in order to assess their explanative information and possible redundancy (Figure 10). The PCA of positive ion data could discriminate bacterial types but not strains regardless of scaling or number of components. The negative ion mode data appeared to contain more information for strain differentiation. The largest variation in both data sets appeared to arise from characteristic contributions of *P. aeruginosa*.

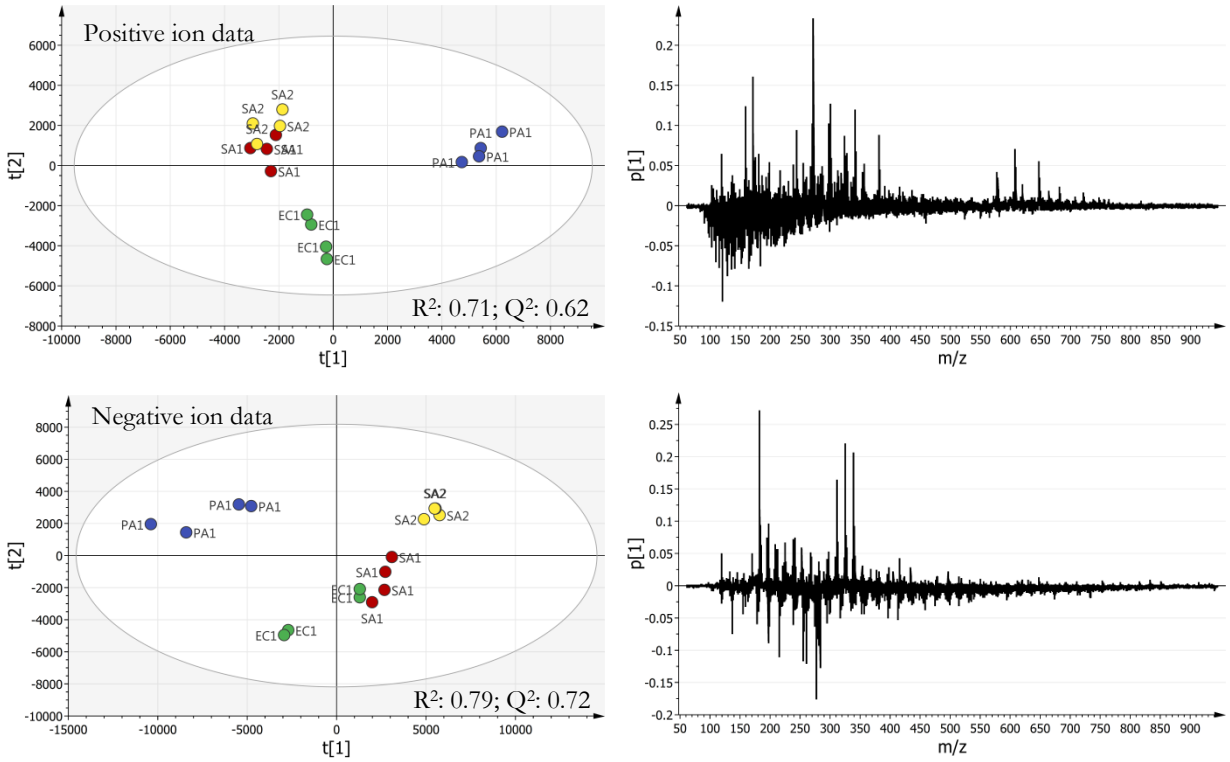

Figure 10. PCA scores and loadings for examining positive and negative ion mode data separately. Pareto scaled PCA with two principal components each; green: *E. coli*; blue: *P. aeruginosa*; red and yellow: two strains of *S. aureus*.

Combining positive and negative ion mode data resulted in full separation of all test strains using the first two or three most significant principal components depending on the scaling method (Figure 11). Cluster separation improved with scaling method from no scaling, to Pareto, to UV scaling. In contrast, the interpretability of loadings decreased in the same order. A PCA with Pareto scaling showed cluster separation and interpretable loadings.

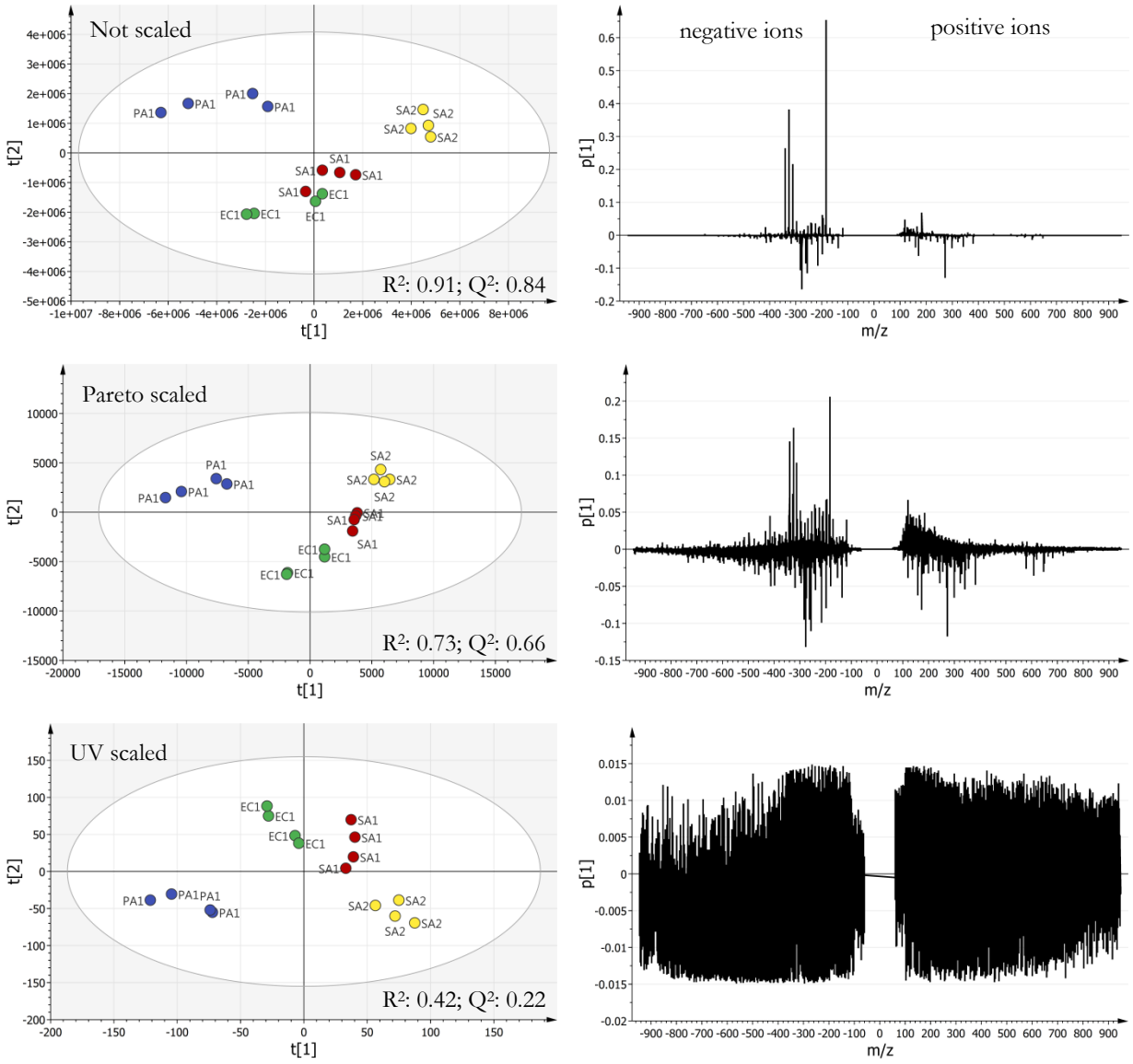

Figure 11. Comparison between the effects of scaling methods on PCA scores and loadings of combined data from positive and negative ion mode spectra. PCA with two principal components each; green: *E. coli*; blue: *P. aeruginosa*; red and yellow: two strains of *S. aureus*.

5.2.2 Elucidation of extra cellular signaling molecule by MSMS

Collision induced dissociation of *m/z* 272 yielded strong product ions at *m/z* 159 and 172 (Figure 12). This confirmed that the three largest loading peaks in PC p1 arose from the same compound, separating *P. aeruginosa* from the other strains. Lépine *et al.* studied 4-hydroxy-2-alkylquinolines (HAQs) produced by *P. aeruginosa* and reported *m/z* 272 with its fragment ions at *m/z* 172 and 159.[128] HAQs have been associated with bacterial virulence and are used by *P. aeruginosa* as extra cellular signaling molecules in quorum sensing (see also *Section 1.3.2*).[128] Extra cellular molecules may remain on the surface of the cell samples and are thus likely to be detected by ToF-SIMS.

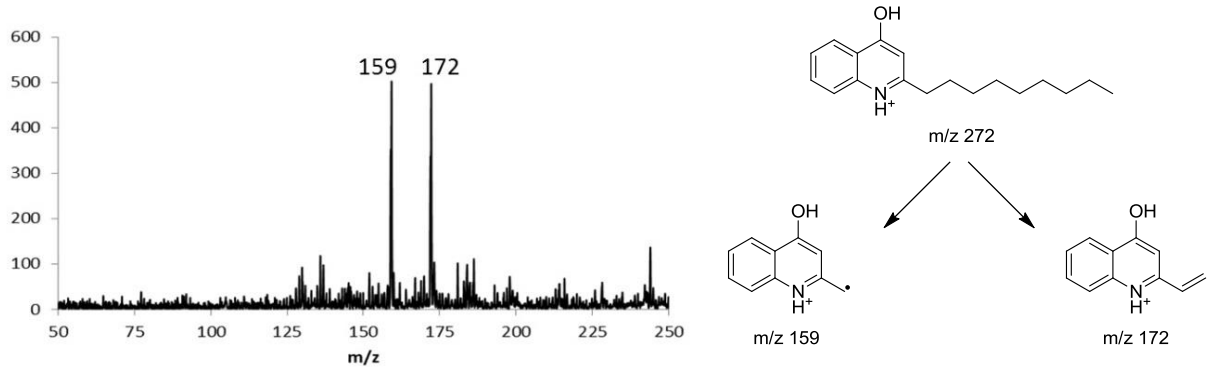

Figure 12. MSMS Fragment spectrum produced by high energy CID of *m/z* 272 in positive ion mode. Putative structures of *m/z* 272 and its fragment ions produced by CID of the $[M+H]^+$.

5.3 Investigating the role of the stringent response in lipid modifications upon starvation in *E. coli* (Paper IV)

When *E.coli* bacteria encounter nutrient limitation, they rapidly adjust their metabolic activities in order to promote survival through the starvation period.[129, 130] Much of this regulation is *via* the stringent response which further regulates virulence traits and has been linked to persistence and drug tolerance.[16, 131, 132] The problem of bacterial persistence and resistance to antibiotics demands not only the development of new drugs and drug targets, but also a better understanding of bacterial physiology in persistence and stress response. In this study, changes in membrane lipids as a result of adaptation to starvation stress in *E. coli* were investigated by direct analysis with ToF-SIMS. A mutant strain of *E. coli,* deficient in the stringent response, was included to link observed changes to underlying metabolic pathways.

5.3.1 The stringent response

Bacteria have evolved sophisticated stress response mechanisms that allow them to adapt to environmental challenges including nutrient limitation and starvation.[129, 130] These adaptations depend on complex regulatory mechanisms, such as the stringent response, a bacterial global gene regulation system. The stringent response is triggered by various nutritional stress cues and functions by rapidly reprogramming transcription to adapt metabolism and protein composition to ensure survival through the starvation period.[133] The effector molecule of the stringent response is the unusual nucleotide guanosine tetraphosphate (ppGpp). When *E. coli* bacteria face nutrient starvation, their intracellular concentration of ppGpp increases by the synthetic action of the RelA and SpoT enzymes (ppGpp synthetases I and II).[13, 36, 134] RelA is thought to act specifically in response to amino acid limitation, whereas SpoT is activated upon various stress signals, including carbon, phosphate, iron and fatty acid starvation.[135] As a pleiotropic stress response regulator, ppGpp modulates the transcription of hundreds of genes[136, 137] and plays a key role, not only in starvation survival, but also in biofilm formation, regulation of virulence, drug tolerance, and persistence.[13, 36, 132, 135] High levels of ppGpp have been linked to increased persister cell formation, whereas deficiency in ppGpp production *via* deletion of the *relA* and *spoT* genes (coding for ppGpp synthetases I and II, respectively) resulted in much rarer occurrence of persister cells in exponentially grown planktonic cultures.[20, 22, 138, 139] Finally, ppGpp mediates low metabolic activity including slow growth which is associated with persistence and drug tolerance and links the stringent response to recalcitrance to antibiotic therapy.[16, 22, 131] Due to its pivotal role in both persistence and virulence, the stringent response has been investigated as potential target for anti-infective therapy.[135, 140]

5.3.2 Multivariate data overview

Cultures of wild-type *E. coli* K-12 and a ppGpp^0 mutant (Δ*relA*::kan Δ*spoT*::cam, deficient in production of ppGpp) strain were grown with glucose as limiting substrate and

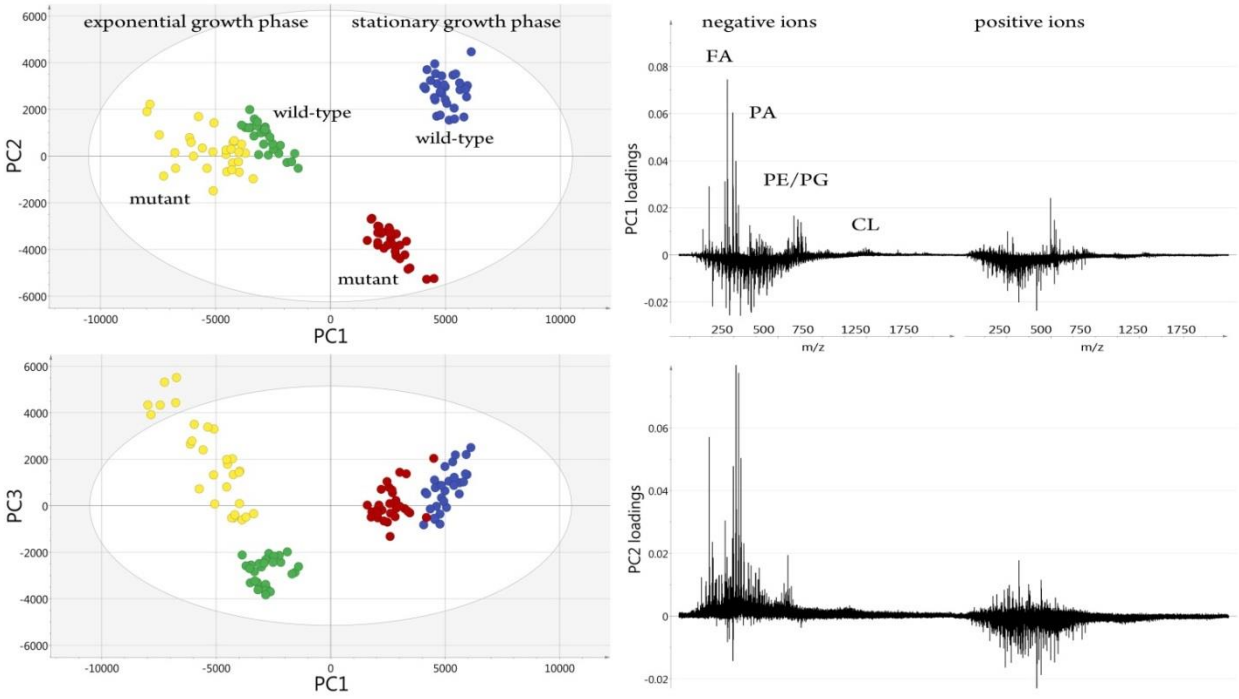

Figure 13. PCA scores and loadings of ToF-SIMS spectral data obtained from wild-type *E. coli* and its ppGpp^0 mutant (Δ*relA*Δ*spoT*) strain (Pareto-scaled and mean-centered, $R^2 = 0.53$; $Q^2 = 0.50$; Ellipse: 95% confidence region). Annotations on the loadings plot refer to fatty acids (FA), phosphatidic acids (PA), phosphatidylethanolamines (PE), phosphatidylglycerols (PG), cardiolipins (CL).

analyzed with ToF-SIMS in exponential and stationary growth phase. PCA of the mass spectral data, shown in Figure 13, was used to examine the data structure. The PCA model with Pareto-scaling separated all four different sample types using the first three most significant principal components ($R^2 = 0.53$; $Q^2 = 0.50$). The largest variation (PC1) appears to arise from growth phase specific lipid differences. The strains in stationary growth phase are separated along PC2 due to differences caused by altered lipid modification arising from their genetic variation. Finally, the strains in exponential phase share most similarities but were distinguished along PC3 based on unassigned differences. Such observations were expected as the *rel*A and *spo*T genes involved in the stringent response are of lesser importance in the absence of starvation stress. The differences described by the PCA loadings are discussed in further detail in the following sections.

5.3.3 Mass spectral assignment overview

Assignment of mass spectral peaks provided insight into the specific differences that ultimately allowed one to draw conclusions about the underlying metabolic pathways. Assignments include variants of fatty acids (FA), phosphatidic acids (PA), phosphatidylethanolamines (PE), phosphatidylglycerols (PG), and cardiolipins (CL), and are supported by positive and negative ion mode data, fragmentation patterns, high mass accuracy and previously published data.[141-152] Further confidence in the assignments is provided by logical structural links between assignments as further explained in Figure 14.

A complete list of assigned molecular species and an example spectrum may be found in the appendices (*Appendix 8.8* and *8.9*). The applied nomenclature e.g. PG(cp35:0) allows direct comparison between the different types of phospholipids. The designation within parentheses refers to structural features (e.g. cp for cyclopropane), the number of carbons within the fatty acyl substituents (e.g. 35), and to the number of unsaturations within the acyl chains (e.g. 0).

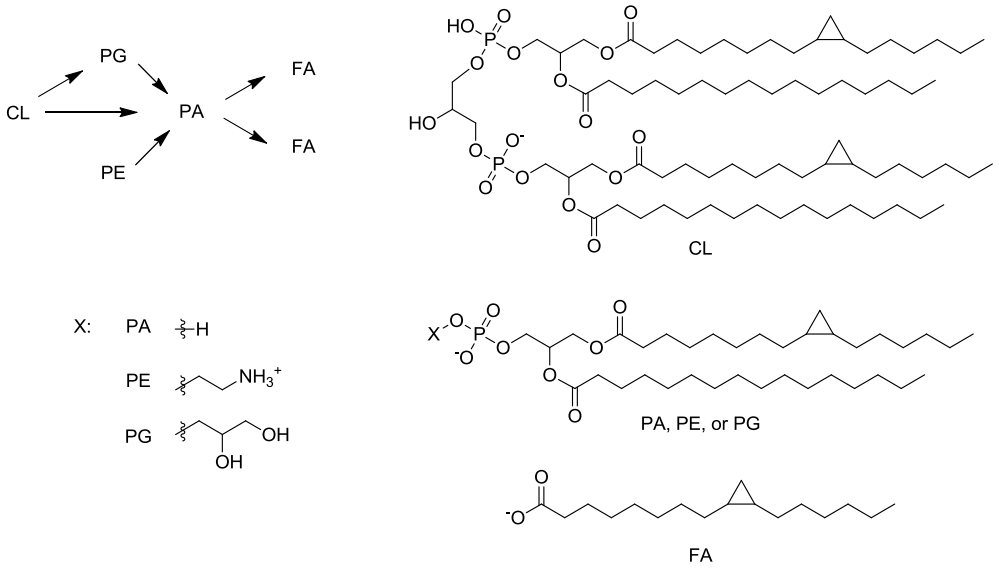

Figure 14. Fragmentation during ion generation gives rise to a structural relationship between observed ions. This increases confidence in assignments of structural analogues and the exclusion of unrelated structures with isobaric interference. The schematic shows possible fragmentation yielding classes of smaller ions e.g. by the loss of the head group. As a consequence of fragmentation, it is uncertain which or how much of the species are actually present in the sample. Structures are shown as examples, whereby the conformational kink introduced by cp is not illustrated.

5.3.4 Membrane lipid composition in exponential growth phase.

Both, wild-type *E. coli* and the ppGpp^0 mutant in exponential phase were found to primarily have saturated fatty acids and phospholipids incorporated in their membranes. Mass spectral assignments identified the fatty acids FA(16:0), FA(14:0), FA(12:0) and FA(10:0), as well as the phospholipids PG(28:0) and PG(26:0), including their PE and PA analogues. The evenly numbered acyl chains can be explained by the mechanism of fatty acid synthesis which applies two-carbon building blocks in an iterative process.[153, 154] Interestingly, these saturated phospholipids appear to have a complete set of hydroxylated analogues. However, only the hydroxy fatty acids FA(OH-10:0) and FA(OH-12:0) were detected. Signals corresponding to FA(OH-14:0) and FA(OH-16:0) fatty acids were not observed. Therefore, it remains unclear whether hydroxy phospholipids are an artifact of our analysis procedure or could be detected due to analyzing native samples. The assignment of hydroxy phospholipids

is tentative, nevertheless, most assignments from exponential growth are consistent in their structural relationship and are supported by previous studies.[145, 149, 150, 152]

5.3.5 Membrane lipid composition in stationary growth phase of wild-type *E. coli*.

The lipid composition of *E. coli* in stationary phase was found to be radically different as compared to exponentially grown cells. The starved cells appeared to have modified their membrane lipids by elongation and cyclopropanation of their pre-existing[153] fatty acyl chains. As a result, the majority of dominant peaks were attributable to cyclopropane containing species of FA, PA, PE, PG, and CL. Cyclopropane containing lipids have previously been described as physiologically useful as they confer increased resistance to environmental insults such as acid stress.[155] Further, the cp ring affects the confirmation of the acyl chain by the introduction of a kink, resulting in less dense lipid packing and in turn, in an increase in the membrane's fluidity.[153] The cp containing fatty acids FA(cp17:0) and FA(cp19:0) gave rise to the most intense peaks in the negative ion mode mass spectrum. Due to their high abundance, their positive ion counter parts were tentatively assigned to the unusual positive ions $[FA+26]^+$ (*Appendix 8.10*). Further peaks consistent with fatty acids were assigned to FA(14:0), FA(16:1), FA(16:0), and FA(18:1). The largest peaks attributable to phospholipids were assigned to PG(cp33:0), PG(cp35:0) and their PE and PA analogues. CL levels increased strongly during stationary phase, whereby only cp containing CL species were observed. CL can be formed by condensation of two PGs, or PG and PE by CL synthase (Cls)[156, 157] The activity of Cls has been reported to increase 10-fold when entering stationary phase, which supports our observation.[158] Further, CL are crucial for viability in long-term stationary phase.[156]

The time point in the growth curve in which a planktonic culture of *E. coli* is sampled is critical to the types of lipids that can be detected, and should to be considered when sampling any type of bacterium. The modification of phospholipids appeared to progress, even during the stationary phase itself, as found serendipitously. In early stationary phase, phospholipids exhibiting one cp ring were observed, and as cyclopropanation continued, species with two cp rings began to appear (as illustrated in Figure 15A and B). This time dependent appearance suggests that existing phospholipids are modified.[153]

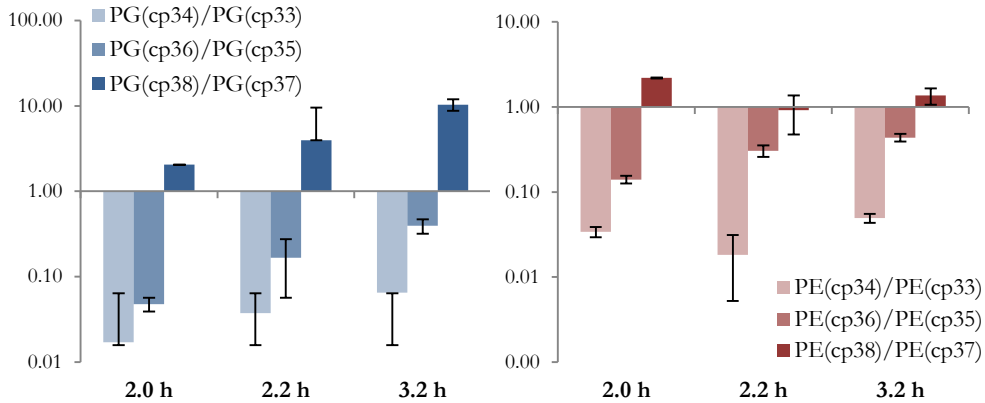

Figure 15A. Ratios of doubly to singly cyclopropanated PG and PE in wild-type *E. coli* over time in the stationary phase. Error bars show standard deviation (n = 6).

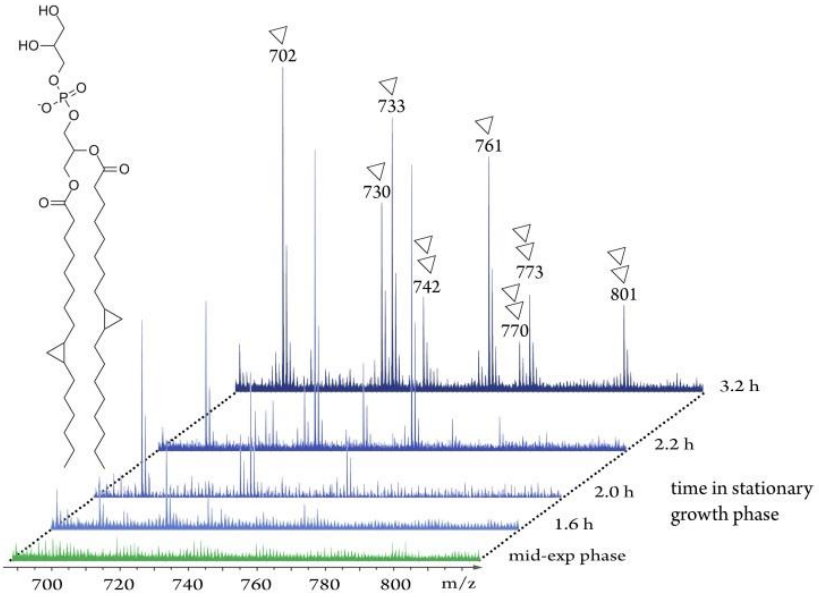

Figure 15B. ToF-SIMS spectra to illustrate the time-dependent lipid modification in stationary phase of wild-type *E. coli*. First, phospholipids with a single cp ring are detected and as cyclopropanation progresses also species with two cp rings appear. The example structure is consistent with *m/z* 733. Spectra are normalized based on noise levels.

5.3.6 Anomalies in the phospholipid modifications of ppGpp^0 mutant *E. coli* in stationary phase.

The lipid profile of the ppGpp^0 mutant in exponential growth phase was very similar to that of the wild-type. This was expected as ppGpp is not synthesized significantly during exponential growth and, therefore, lack of the genes coding for ppGpp synthases would not affect homeostasis noticeably. In stationary phase, however, wild-type *E. coli* elicits the stringent response by expression of *relA* and/or *spoT* leading to production of ppGpp. Resulting phospholipid modifications yielded cp containing lipids which were observed exclusively in wild-type cells. Interestingly, the ppGpp^0 mutant in stationary phase was found to have a complete set of unsaturated analogues of these cp lipids instead (Figure 16). The observed ions are consistent with PG(34:1), PG(32:1), PE(34:1), PE(32:1), PA(34:1), PA(32:1), FA(18:1), and FA(16:1). This was somewhat unexpected as the relaxed response yields a proteomic profile[159] as well as a gene expression profile[160] in stationary phase similar to that during growth.[13] Like the wild-type, the ppGpp^0 mutant responds to starvation stress with elongation and desaturation of pre-existing fatty acyl chains. However, in the wild-type, ppGpp stimulates accumulation of the RpoS regulon which controls the *cfa* gene encoding cyclopropane fatty acid synthase (Cfa). Cfa is required for the subsequent methylation of the double bond to form cyclopropane moieties.[153] Deletion of the genes encoding RelA and SpoT renders the mutant strain deficient in production of ppGpp which leads to an altered

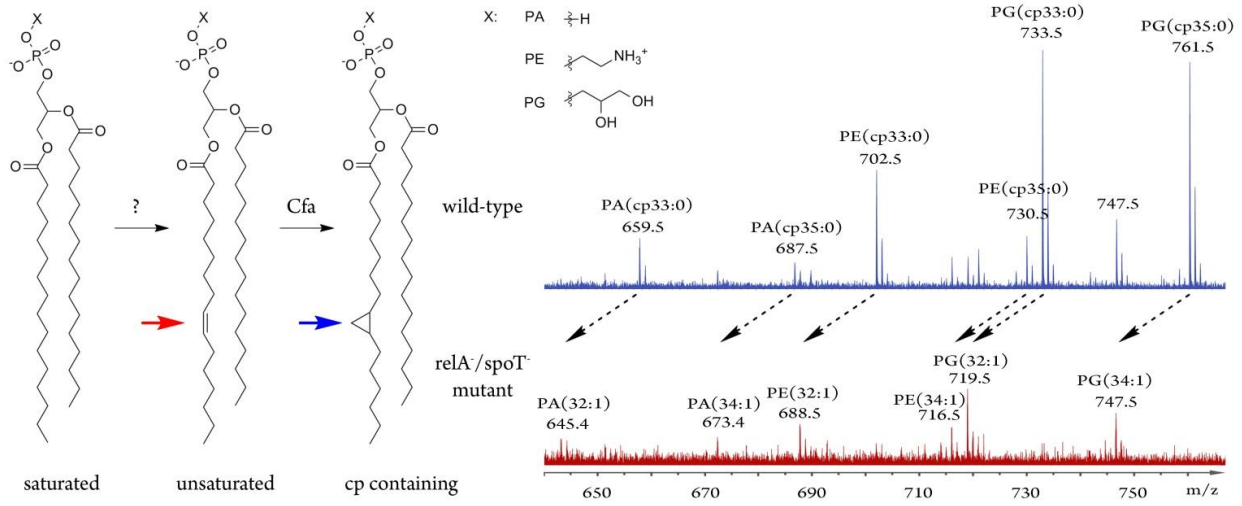

Figure 16. Lipid modifications in the stationary growth phase of wild-type *E. coli* and its ppGpp^0 mutant strain include elongation and desaturation of preexisting phospholipids, however, only the wild-type is capable of subsequent cyclopropanation by Cfa. As a result, the mutant cells exhibited unsaturated analogues (red spectrum, negative ion mode) of the cp phospholipids found in the wild-type (blue spectrum). The mechanism that introduces the unsaturations is currently unclear. Structures are shown as an example; modifications can occur in Δ^5 or Δ^9 positions. The conformational kink introduced by the modifications is not illustrated.[153]

stress response and incomplete phospholipid modification. The observation of unsaturated analogues suggests that only the last step of the modifications, the cyclopropanation, is under ppGpp control. Further, this may indicate alternative stress response mechanisms, which regulate the membrane lipid structure independently from ppGpp.

It is currently unclear how the observed desaturation occurs in *E. coli*. Other types of bacteria use desaturases to modify their pre-existing phospholipids.[134] However, wild-type *E. coli* does not produce desaturases and has therefore been used to recombinantly express desaturases.[161] In *E. coli*, FabA and FabB are enzymes involved in the formation of double bonds. These enzymes are known to process acyl carrier protein (ACP) linked acyls during *de novo* biosynthesis of fatty acids.[134, 153] The data from this study suggest, however, that the modification occurs on pre-existing phospholipids rather than by *de novo* synthesis. Also the transcriptional regulation of the *fabA* and *fabB* genes indicates that the desaturation occurs by another mechanism. The *fabA* gene is repressed in starvation[162, 163] and *fabB* is shown to be downregulated during amino acid starvation[164] while induced in the stationary phase in LB medium.[162] While the underlying mechanism of the observed unsaturations is poorly understood, our results suggest that the biosynthesis of the enzyme(s) involved in desaturation is not regulated by ppGpp.

The absence of signals corresponding to unsaturated CL analogues in the ppGpp^0 mutant cells might suggest that Cls activity is ppGpp dependent. This, however, remains speculative and could also be due to low intensity.

5.3.7 Implications of lipid structure alterations in cell morphology and membrane homeostasis

The molecular alterations of the lipid structure, described above, may contribute to the morphological differences between the cells observed in brightfield microscopy (Figure 17). The similar lipid profiles of the wild-type and the ppGpp^0 mutant in exponential growth phase were accompanied by a close resemblance in the appearance of their rod-shaped cells (Figure 17A and B, respectively). In the stationary phase, wild-type *E. coli* appears to make further restrictions to form small, almost spherical cells that segregate in to a large number of cells — a strategy which may increase the chance of survival (Figure 17C). Thereby, the high curvature of the cells may be allowed by the increased CL content in their membranes. Previously, CL domains have been associated with regions of high cell curvature and have been localized to the cell poles as well as at division sites.[157] The significant increase in cp lipid species may further contribute to the curved shape, which is speculative and remains to be investigated. The ppGpp^0 mutant fails to become coccoid in stationary phase and forms

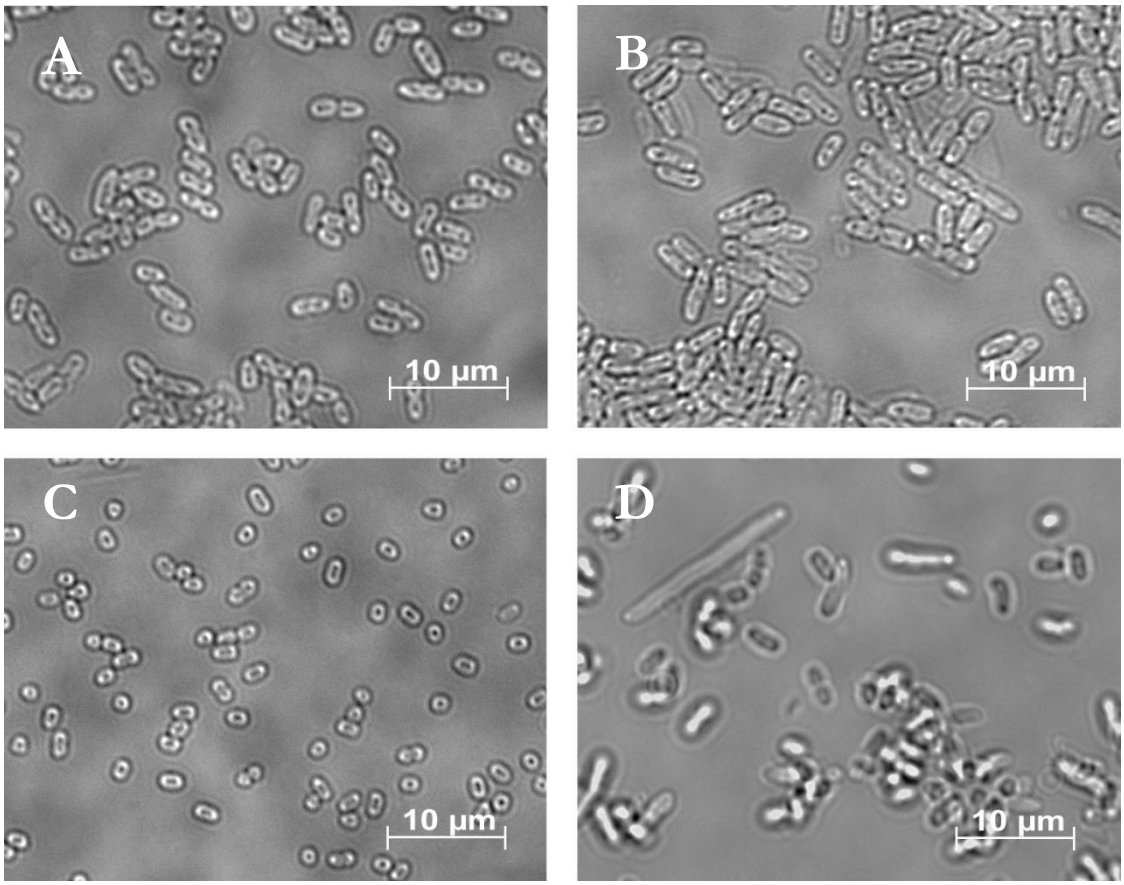

Figure 17. Brightfield microscopy images of *E. coli* wild-type and its ppGpp^0 mutant (ΔrelAΔspoT) strain in mid-exponential growth phase (A and B, respectively), and during stationary phase (C and D, respectively). The images were captured slightly defocused to enhance contrast, using a Zeiss Axiovert 200M inverted microscope equipped with a 100× plan apochromat (NA 1.4) oil immersion objective.

filaments and pear-shaped cells instead (Figure 17D).[165] The lipid structures might contribute to a certain part to the odd cell shapes, however, deletion of a global gene regulation system, such as the stringent response, may have far reaching implications.

It has previously been established that the structural integrity and function of membrane proteins are affected by their lipid environments.[157, 166] The growth condition dependent lipid composition may, therefore, affect the binding affinity of drug molecules to membrane proteins.[166] Moreover, the membrane permeability may change based on its composition, which might affect the target engagement of antibiotics and thereby further complicate the search for new drug-like molecules that effectively penetrate the bacterial barrier. A comprehensive understanding of compound penetration in bacteria to guide the development of synthetic antimicrobials still remains to be established.[167]

It has been shown that environmental parameters affect the membrane fatty acid composition and also the sensitivity to Gentamycin of *Staphylococcus lugdunensis*.[108] The role of lipids in modulating protein function has yet to be fully understood.

5.4 Summary of Paper III and IV

ToF-SIMS in conjunction with MVA was applied for direct and untargeted analysis of various bacterial types and strains. In an initial study, a set of four bacteria was distinguished down to the strain level. MSMS data provided information that allowed the identification of an extra cellular signaling molecule of *P. aeruginosa*. In a subsequent study, membrane lipid modifications as a result of adaptation to starvation stress in *E. coli* were investigated and compared to a $ppGpp^0$ mutant strain, deficient in the stringent response. The two strains shared strong similarities in exponential growth phase, regarding ToF-SIMS spectra, lipid composition and cell morphology. In stationary phase, the cells appeared to have undergone radical changes in the lipid structure, resulting in the wild-type in cyclopropanated lipids and largely increased CL levels. In contrast, the $ppGpp^0$ mutant cells were found to exhibit unsaturated analogues of lipids found in the wild-type. This indicates that only the last step of the lipid modification, the cyclopropanation, is under stringent control and further suggests ppGpp independent stress response mechanisms.

6 CONCLUDING REMARKS AND FUTURE PERSPECTIVES

This thesis describes firstly the discovery, synthesis and evaluation of inhibitors of SrtA, and secondly the phenotypic characterization of bacteria using FTIR spectroscopy and ToF-SIMS. FTIR spectroscopy in combination with DOE and MVA was found to be a powerful tool for the investigation of phenotypic diversity of *S. aureus*. ToF-SIMS in conjunction with MVA was shown to be capable of differentiating a number of bacterial strains. Further investigations with ToF-SIMS included starvation experiments, which revealed ppGpp independent lipid modifications in *E. coli*.

Further studies that would be of interest include:

- The impact of ToF-SIMS surface sampling on bacterial cells is currently unclear. Scanning electron microscopy may be applied to gain insight in sample surface alterations of primary ion beam(s). Furthermore, it may be attempted to resolve differences between the inner and the outer membranes of Gram-negative bacteria by 3D chemical imaging.

- ToF-SIMS may be applied for the investigation of small colony variants (SCV), which due to the low amount of sample are challenging to analyze with other methods.

- ToF-SIMS maybe applied to further investigate lipid modifications of *E. coli* mutants (e.g. *cfa* deletion, *hipA* overexpression) to gain insight in persister cell physiology.

- CFA phospholipids may contribute to cell curvature. It could be of interest to localize CFA lipids to curved regions (poles) of exponentially growing *E. coli* using Nano-SIMS.

7 ACKNOWLEDGEMENTS

I would like to thank my legs, for supporting me, my arms for always being by my side. And my fingers – I could always count on them. I would like to express my deepest gratitude to all the following people, who have all given me their support in one way or the other, during these years:

First of all my supervisor, **Johan Gottfries**, for accepting me as your doctoral student, for your guidance, for your openness towards ideas, for your trust in me and for letting me work with such great freedom.

My examiner, **Katrina Abrahamson** for the giving talks and your advice.

Many special thanks go to **Thomas Olsson**, for the interesting discussions, for sharing your knowledge, guiding us, and supporting us with so many things. It was invaluable to have you in our team.

John Fletcher, for a very valuable collaboration, great scientific discussions, and teaching me so much about your shiny instrument.

To **Tina Seifert**, thank you for the good discussions, your chemistry advice and your hospitality. It was great to work in the lab with you.

Ivana Uzelac, for the chats and discussions, the team work and sharing your positive way of dancing through life.

Tina Angerer, thank you for the chats and discussions, for the collaborations and lab work.

Many thanks to **Erika Lundberg**, collaborator microbiology, for a very valuable collaboration, the helpful discussions and advice, and the many experiments you helped to realize.

Anne Farewell, collaborator molecular biology, thank you for sharing your expertise, every time we met you taught me something new.

Jonas Eriksson, thank you for your great hospitality during my stay in Umeå and thank you and **Per-Anders Enquist** for all the advice you shared with me around HTS and assay development.

To **Cecilia Persson**, thank you for your efforts around the NMR studies.

My co-authors of papers, **Mats Josefson**, **Anders Sparén**, **Olof Svensson**, **Anges Wold**, **Hugh Dunstan**, **Tomas Jacso**, **Chunxia Gao**, and **Leif Eriksson** thank you for all the helpful discussions and useful advice.

To all the reviewers of my thesis, **Cassandra**, **Johan**, **Thomas**, **Anne**, thank you very much for taking the time out to review my thesis.

Kristina Luthman, thank you for all your helpful advice and letting me work in your lab.

Patrik Jarvoll, thank you for patiently taking the time out to give me NMR advice and explanations.

Alberte, **Bijan**, **Carlo**, **Patrik** and **Mate** thank you for your efforts to keep the NMR and LCMS instruments running.

Annette and **Nisse**, thank you for your hospitality and letting me work in your labs - that was very valuable.

Thanks to **Esa Väänänen**, mechanic, for helping me build the XY-stage for the FTIR instrument.

Thanks a lot to **Mate Erdelyi** for your efforts to improve courses and your support with the KEM030 app.

Carlo & Gulia, thanks for the fun chats and your friendliness; I would share an office with you anytime.

Thanks to all valuable colleagues associated with the **8th floor**.

All colleagues associated with the **4th** and **5th floor**, thanks for the good times in the breaks.

And to my Swiss and Swedish families thank you for being there for me. Last but not least, my own family, **Linnéa**, **Melinda** and **Melody**, it was great to feel your love and support.

8 APPENDICES

8.1 Appendix 1.

8.2 Appendix 2.

8.3 Appendix 3.

8.4 Appendix 4. FTIR instrumental setup

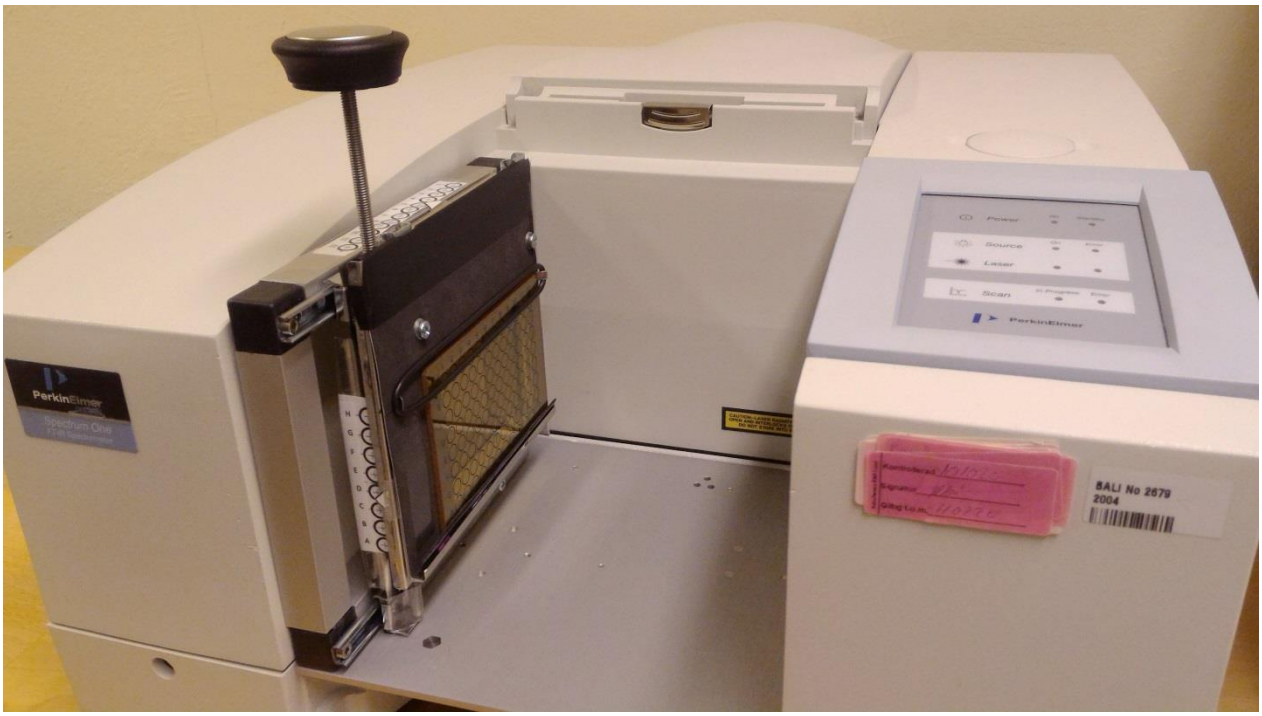

Figure A1. FTIR spectrometer with custom built xy-stage holding a ZnSe well plate as it was used to acquire FTIR spectra of bacterial samples.

8.5 Appendix 5. FTIR optical substrate comparison

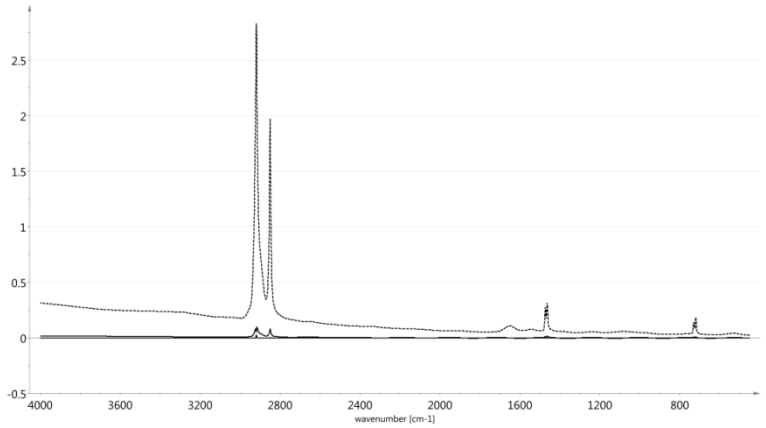

Figure A2. Solid line spectra show replicate measurements of blank Polyethylene (M3) as optical windows, dashed spectra show a bacterial spectrum for relative comparison.

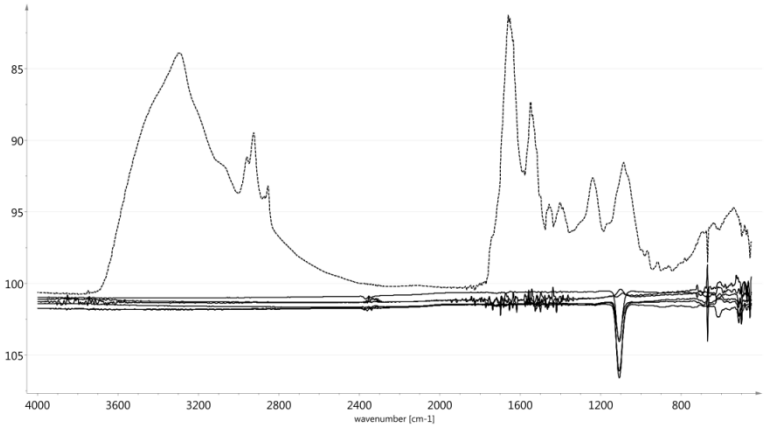

Figure A3. Solid line spectra show replicate measurements of blank Silicon waver as optical windows, dashed spectra show a bacterial spectrum for relative comparison.

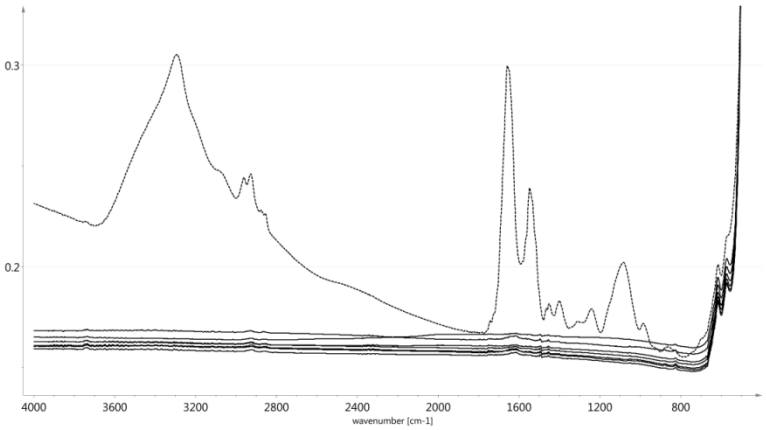

Figure A4. Solid line spectra show replicate measurements of blank individual ZnSe windows as optical windows, dashed spectra show a bacterial spectrum for relative comparison**.**

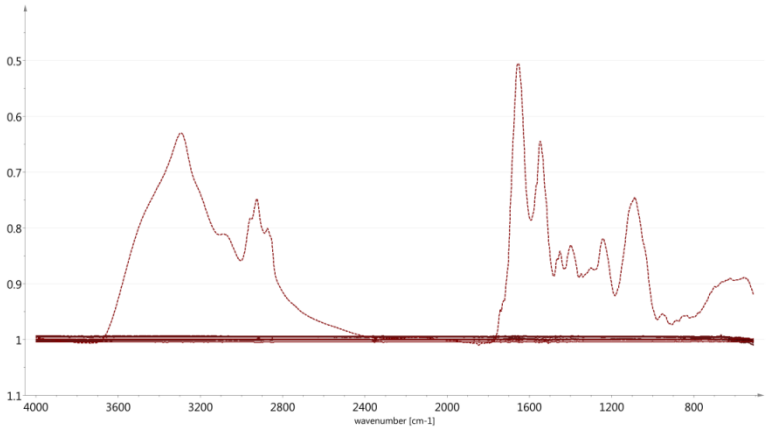

Figure A5. Solid line spectra show replicate measurements of blank ZnSe well plate optical windows, dashed spectra show a bacterial spectrum for relative comparison.

8.6 Appendix 6. PCA scores plot PC6 vs PC3

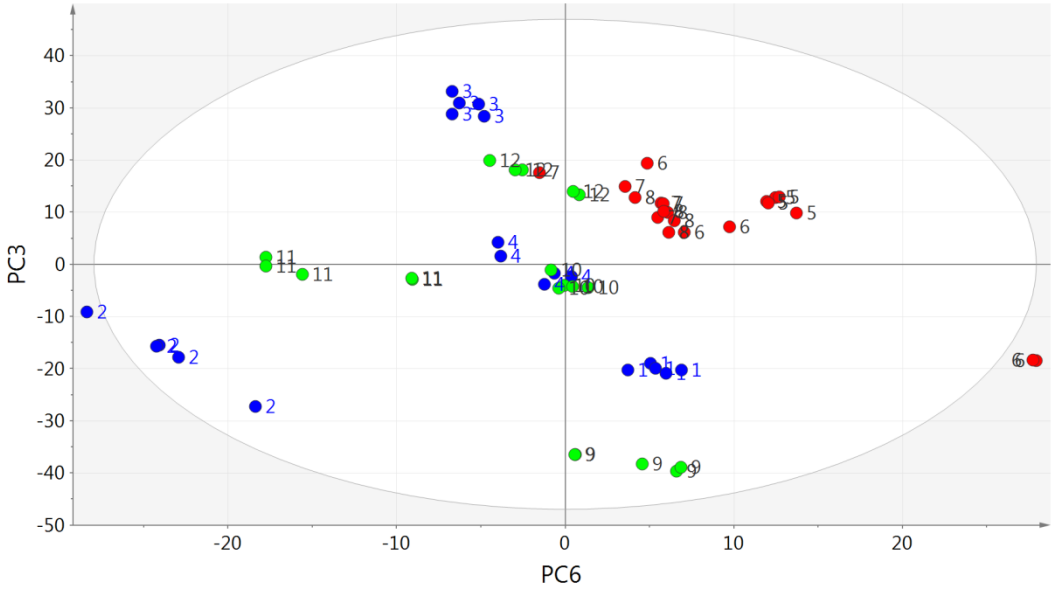

Figure A6. PCA scores plot PC6 vs PC3. Slight separation of high temparature samples could be assumed along PC6. UV scaled; red: high temperature; green: intermediate temperature; blue: low temperature.

Table A1. PCA model details

Component	R2X	R2X(cum)	Eigenvalue	Q2	Q2(cum)	Significance
0	Cent.					
1	0.43	0.43	25.8	0.418	0.418	R1
2	0.169	0.599	10.2	0.261	0.57	R1
3	0.13	0.729	7.78	0.306	0.702	R1
4	0.0806	0.81	4.84	0.25	0.776	R1
5	0.0498	0.86	2.99	0.191	0.819	R1
6	0.0459	0.905	2.75	0.304	0.874	R1
7	0.0301	0.936	1.81	0.282	0.909	R1
8	0.0172	0.953	1.03	0.233	0.931	R1
9	0.0113	0.964	0.679	0.175	0.943	R1

8.7 Appendix 7. OPLS model

Table A2. OPLS model details

Component	R2X	R2X(cum)	Eigenvalue	R2	R2(cum)	Q2	Q2(cum)	R2Y	R2Y(cum)	EigenvalueY	Significance
Model		0.955			0.947		0.908		1		
Predictive		0.575			0.947		0.908		1		
P1	0.326	0.326	19.5	0.274	0.274	0.201	0.201	0.282	0.282	1.41	R1
P2	0.153	0.478	9.15	0.335	0.609	0.302	0.503	0.341	0.623	1.71	R1
P3	0.0447	0.523	2.68	0.203	0.812	0.225	0.727	0.225	0.848	1.13	R1
P4	0.0403	0.563	2.42	0.0855	0.898	0.129	0.856	0.0949	0.943	0.474	R1
P5	0.0116	0.575	0.696	0.0493	0.947	0.0519	0.908	0.057	1	0.285	R1
Orthogonal in X(OPLS)		0.38			0						
O1	0.17	0.17	10.2	0	0						R1
O2	0.072	0.242	4.32	0	0						R1
O3	0.0752	0.317	4.51	0	0						R1
O4	0.0365	0.353	2.19	0	0						R1
O5	0.0264	0.38	1.59	0	0						R1

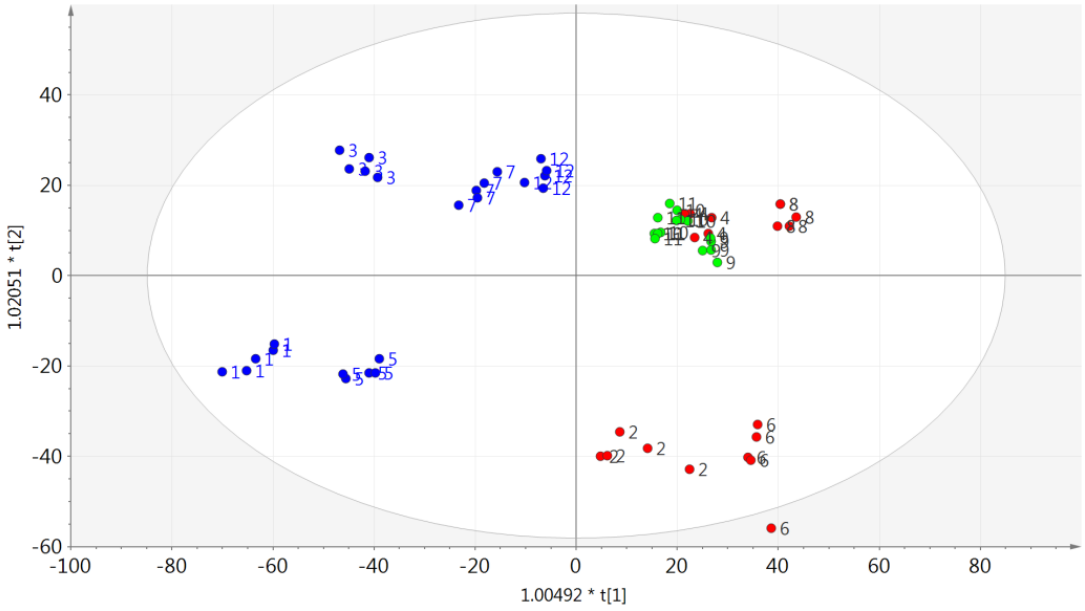

Figure A7. OPLS scores plot pc1 vs pc2. Blue: low salinity; Red: high salinity; Green: intermediate salinity.

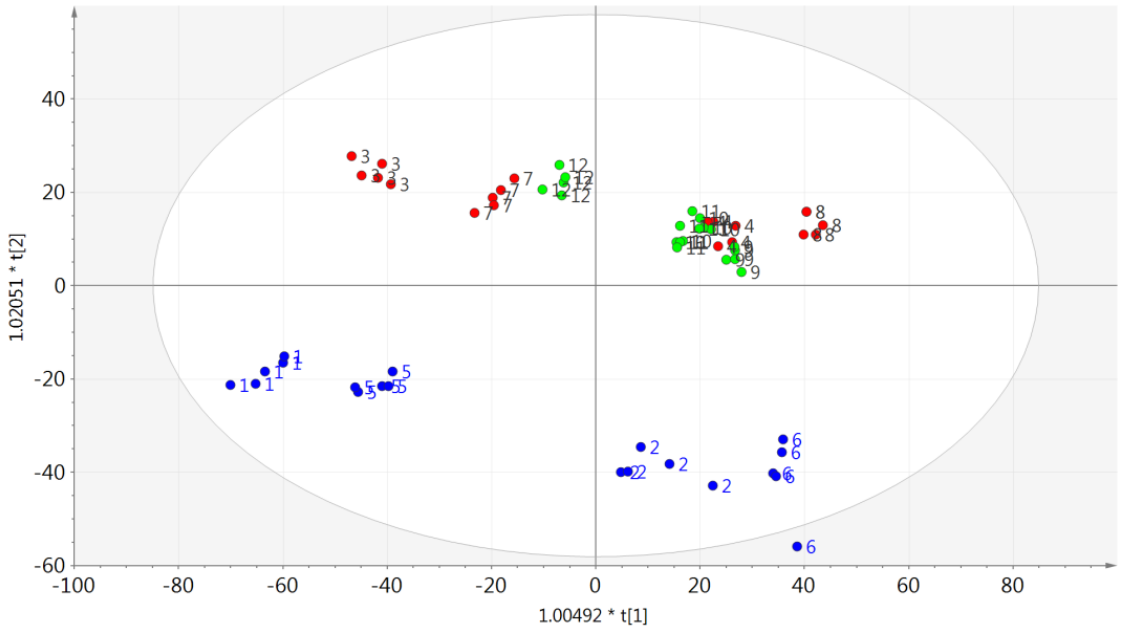

Figure A8. OPLS scores plot pc1 vs pc2. Blue: low pH; Red: high pH; Green: intermediate pH.

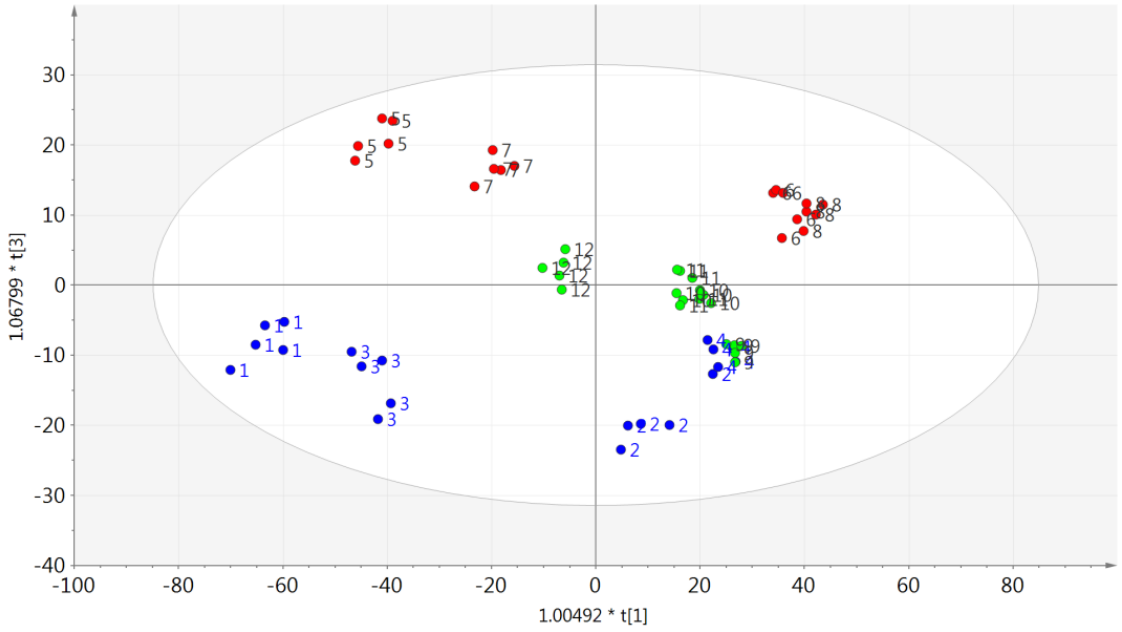

Figure A9. OPLS scores plot pc1 vs pc3. Blue: low temperature; Red: high temperature; Green: intermediate temperature.

8.8 Appendix 8. ToF-SIMS spectral assignments

Table A3. Assignments of signals observed in ToF-SIMS spectra of wild-type and ppGpp^0 mutant *E. coli* in exponential and stationary growth phase.

	Negative ion mode		Positive ion mode		
Assignment	meas. *m/z* [M-H]-	Ion formula	meas. *m/z*	Species	Ion formula
Head groups and fragments					
	78.9	PO_3^-	-	-	-
Dihydrogenphosphate	96.9695	$H_2PO_4^-$	-	-	-
	134.9848	$C_3H_4O_4P^-$	-	-	-
	137.0029	$C_3H_6O_4P^-$	-	-	-
Phosphoethanolamine	140.0136	$C_2H_7NO_4P^-$	-	-	-
	152.9975	$C_3H_6O_5P^-$	-	-	-
	158.926	$HP_2O_6^-$	-	-	-
Phosphoglycerol	171.0076	$C_3H_8O_6P^-$	-	-	-
Pyrophosphate	176.9394	$H_3P_2O_7^-$	-	-	-
	196.0387	$C_3H_5OPO_4CH_2$ $CH_2NH_2^-$	-	-	-
Fatty acids					
FA (10:0)	171.1084	$C_{10}H_{19}O_2^-$	-	-	-
FA (OH-10:0)	187.1	$C_{10}H_{19}O_3^-$	-	-	-
FA (12:1)	197.1194	$C_{12}H_{21}O_2^-$	-	-	-
FA (12:0)	199.1348	$C_{12}H_{23}O_2^-$	-	-	-
FA (OH-12:0)	215.1294	$C_{12}H_{23}O_3^-$	-	-	-
FA (14:0)	227.2005	$C_{14}H_{27}O_2^-$	-	-	-
FA (16:1)	253.2154	$C_{16}H_{29}O_2^-$	-	-	-
FA (16:0)	255.2323	$C_{16}H_{31}O_2^-$	282.2559	$[FA+26]^+$	$C_{18}H_{34}O_2^{\bullet+}$
FA (cp17:0)	267.2328	$C_{17}H_{31}O_2^-$	294.2561	$[FA+26]^+$	$C_{19}H_{34}O_2^{\bullet+}$
FA (18:1)	281.2476	$C_{18}H_{33}O_2^-$	308.2746	$[FA+26]^+$	$C_{20}H_{36}O_2^{\bullet+}$
FA (cp19:0)	295.2640	$C_{19}H_{35}O_2^-$	322.2894	$[FA+26]^+$	$C_{21}H_{38}O_2^{\bullet+}$
Phosphatidic acids					
PA (26:0)	563.3406	$C_{29}H_{56}O_8P^-$	467.4019	$[M+H-98]^+$	$C_{29}H_{55}O_4^+$
PA (OH-26:0)	579.3196	$C_{29}H_{56}O_9P^-$	483.3837	$[M+H-98]^+$	$C_{29}H_{55}O_5^+$
PA (28:0)	591.3553	$C_{31}H_{60}O_8P^-$	495.4194	$[M+H-98]^+$	$C_{31}H_{59}O_4^+$
PA (OH-28:0)	606.37	$C_{31}H_{59}O_9P^-$	-	-	-
PA (30:0)	619.4033	$C_{33}H_{64}O_8P^-$	523.4854	$[M+H-98]^+$	$C_{33}H_{63}O_4^+$
PA (OH-30:0)	635.3829	$C_{33}H_{64}O_9P^-$	-	-	-
PA (32:1)	645.4574	$C_{35}H_{66}O_8P^-$	549.5043	$[M+H-98]^+$	$C_{35}H_{65}O_4^+$
PA (cp33:0)	659.467	$C_{36}H_{68}O_8P^-$	563.5035	$[M+H-98]^+$	$C_{36}H_{67}O_4^+$

PA (34:2)	-	-	575.5015	$[M+H-98]^+$	$C_{37}H_{67}O_4^+$
PA (34:1)	673.4778	$C_{37}H_{70}O_8P^-$	577.5194	$[M+H-98]^+$	$C_{37}H_{69}O_4^+$
PA (cp35:0)	687.4995	$C_{38}H_{72}O_8P^-$	591.5370	$[M+H-98]^+$	$C_{38}H_{71}O_4^+$
PA (cp36:0)	699.4932	$C_{39}H_{72}O_8P^-$	603.5366	$[M+H-98]^+$	$C_{39}H_{71}O_4^+$
PA (cp38:0)	727.5284	$C_{41}H_{76}O_8P^-$	631.5678	$[M+H-98]^+$	$C_{41}H_{75}O_4^+$

Phosphatidylethanolamines

PE (26:0)	606.37	$C_{31}H_{61}NO_8P^-$	467.3890	$[M+H-141]^+$	$C_{29}H_{55}O_4^+$
PE (OH-26:0)	622.3666	$C_{31}H_{61}NO_9P^-$	483.3837	$[M+H-141]^+$	$C_{29}H_{55}O_5^+$
PE (28:0)	634.3988	$C_{33}H_{65}NO_8P^-$	495.4194	$[M+H-141]^+$	$C_{31}H_{59}O_4^+$
PE (OH-28:0)	650.3968	$C_{33}H_{65}NO_9P^-$	652.4215	$[M+H]^+$	$C_{33}H_{67}NO_9P^+$
			511.4145	$[M+H-141]^+$	$C_{31}H_{59}O_5^+$
PE (30:0)	662.4624	$C_{35}H_{69}NO_8P^-$	664.4884	$[M+H]^+$	$C_{35}H_{71}NO_8P^+$
			523.4854	$[M+H-141]^+$	$C_{33}H_{63}O_4^+$
PE (OH-30:0)	678.4913	$C_{35}H_{69}NO_9P^-$	-	-	-
PE (32:1);	688.4936	$C_{37}H_{71}NO_8P^-$	690.5148	$[M+H]^+$	$C_{37}H_{73}NO_8P^+$
PE (cp33:0)	702.5097	$C_{38}H_{73}NO_8P^-$	704.5321	$[M+H]^+$	$C_{38}H_{75}NO_8P^+$
			563.5035	$[M+H-141]^+$	$C_{36}H_{67}O_4^+$
			742.4944	$[M+K]^+$	$C_{38}H_{74}KNO_8P^+$
PE (34:2)	714.5061	$C_{39}H_{73}NO_8P^-$	716.5088	$[M+H]^+$	$C_{39}H_{75}NO_8P^+$
PE (cp34:0)	714.5061	$C_{39}H_{73}NO_8P^-$	716.5088	$[M+H]^+$	$C_{39}H_{75}NO_8P^+$
PE (34:1)	716.524	$C_{39}H_{75}NO_8P^-$	718.5441	$[M+H]^+$	$C_{39}H_{77}NO_8P^+$
			577.5194	$[M+H-141]^+$	$C_{37}H_{69}O_4^+$
PE (cp35:0)	730.5421	$C_{40}H_{77}NO_8P^-$	591.5370	$[M+H-141]^+$	$C_{38}H_{71}O_4^+$
			770.5214	$[M+K]^+$	$C_{40}H_{78}KNO_8P^+$
PE (36:2)	742.5395	$C_{41}H_{77}NO_8P^-$	603.5366	$[M+H-141]^+$	$C_{39}H_{71}O_4^+$
PE (cp36:0)	742.5395	$C_{41}H_{77}NO_8P^-$	603.5366	$[M+H-141]^+$	$C_{39}H_{71}O_4^+$
PE (cp38:0)	770.5683	$C_{43}H_{81}NO_8P^-$	631.5678	$[M+H-141]^+$	$C_{41}H_{75}O_4^+$

Phosphatidylglycerols

PG (26:1)	635.3829	$C_{32}H_{60}O_{10}P^-$	465.3890	$[M+H-172]^+$	$C_{29}H_{53}O_4^+$
PG (26:0)	637.3713	$C_{32}H_{62}O_{10}P^-$	467.3890	$[M+H-172]^+$	$C_{29}H_{55}O_4^+$
PG (OH-26:0)	653.3404	$C_{32}H_{62}O_{11}P^-$	483.3837	$[M+H-172]^+$	$C_{29}H_{55}O_5^+$
PG (28:0)	665.4012	$C_{34}H_{66}O_{10}P^-$	495.4194	$[M+H-172]^+$	$C_{31}H_{59}O_4^+$
PG (OH-28:0)	681.3929	$C_{34}H_{66}O_{11}P^-$	511.4145	$[M+H-172]^+$	$C_{31}H_{59}O_5^+$
PG (30:0)	693.4567	$C_{36}H_{70}O_{10}P^-$	523.4854	$[M+H-172]^+$	$C_{33}H_{63}O_4^+$
PG (OH-30:0)	709.4159	$C_{36}H_{70}O_{11}P^-$	-	-	-
PG (32:1)	719.4913	$C_{38}H_{72}O_{10}P^-$	549.5043	$[M+H-172]^+$	$C_{35}H_{65}O_4^+$
PG (32:0)	721.4998	$C_{38}H_{74}O_{10}P^-$	551.5003	$[M+H-172]^+$	$C_{35}H_{67}O_4^+$
PG (cp33:0)	733.5066	$C_{39}H_{74}O_{10}P^-$	563.5035	$[M+H-172]^+$	$C_{36}H_{67}O_4^+$
PG (34:2)	745.5059	$C_{40}H_{74}O_{10}P^-$	575.5015	$[M+H-172]^+$	$C_{37}H_{67}O_4^+$
PG (cp34:0)	745.5059	$C_{40}H_{74}O_{10}P^-$	575.5015	$[M+H-172]^+$	$C_{37}H_{67}O_4^+$
PG (34:1)	747.5205	$C_{40}H_{76}O_{10}P^-$	577.5194	$[M+H-172]^+$	$C_{37}H_{69}O_4^+$

PG (cp35:0)	761.5337	$C_{41}H_{78}O_{10}P^-$	591.5370	$[M+H-172]^+$	$C_{38}H_{71}O_4^+$
PG (36:2)	773.5336	$C_{42}H_{78}O_{10}P^-$	603.5366	$[M+H-172]^+$	$C_{39}H_{71}O_4^+$
PG (cp36:0)	773.5336	$C_{42}H_{78}O_{10}P^-$	603.5366	$[M+H-172]^+$	$C_{39}H_{71}O_4^+$
PG (cp38:0)	801.5586	$C_{44}H_{82}O_{10}P^-$	631.5678	$[M+H-172]^+$	$C_{41}H_{75}O_4^+$
Cardiolipins					
CL (cp65:0)	1363.9178	$C_{74}H_{141}O_{17}P_2^-$	-	-	-
CL (cp66:0)	1375.9391	$C_{75}H_{141}O_{17}P_2^-$	-	-	-
CL (cp67:1)	1389.9347	$C_{76}H_{143}O_{17}P_2^-$	-	-	-
CL (cp68:1)	1401.9524	$C_{77}H_{143}O_{17}P_2^-$	-	-	-
CL (cp86:0)	1404.0054	$C_{77}H_{145}O_{17}P_2^-$	-	-	-
CL (cp69:0)	1416.0159	$C_{78}H_{145}O_{17}P_2^-$	-	-	-
CL (cp69:1)	1417.991	$C_{78}H_{147}O_{17}P_2^-$	-	-	-
CL (cp70:1)	1429.9609	$C_{79}H_{147}O_{17}P_2^-$	-	-	-
CL (cp70:0)	1432.0219	$C_{79}H_{149}O_{17}P_2^-$	-	-	-
CL (cp72:1); CL (71:0)	1444.0205	$C_{80}H_{149}O_{17}P_2^-$	-	-	-
CL (cp73:0)	1473.0373	$C_{82}H_{154}O_{17}P_2^-$	-	-	-
CL (cp74:0)	1484.032	$C_{83}H_{153}O_{17}P_2^-$	-	-	-

8.9 Appendix 9. ToF-SIMS example spectrum

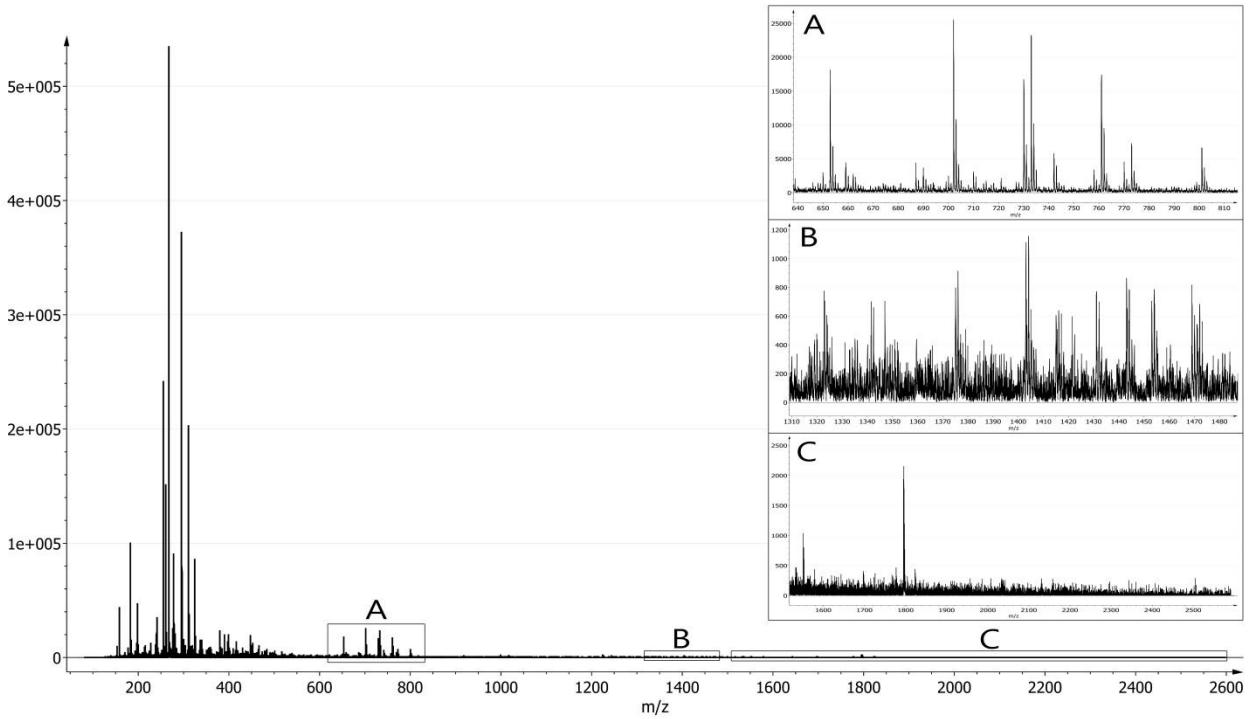

Figure A10. Typical ToF-SIMS spectrum in negative ion mode obtained from wildtype *E. coli* in stationary growth phase.

8.10 Appendix 10. Phospholipid Fragmentation in ToF-SIMS

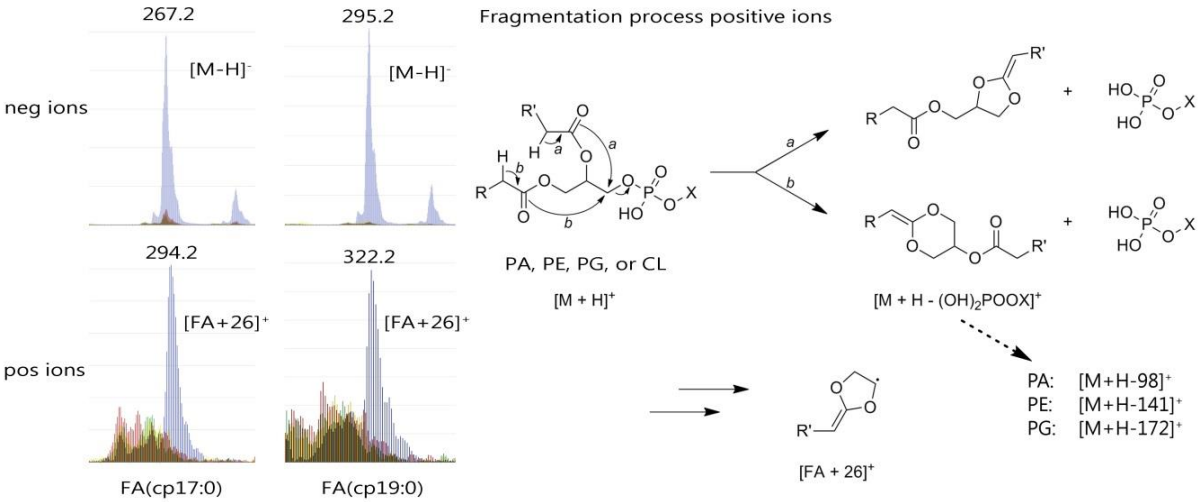

Figure A11. Characteristic abundances of the fatty acids FA(cp17:0) and FA(cp19:0), as assigned *via* negative ion mode data, allowed their assignments also in positive ion mode to $[FA+26]^+$ ions. Fragmentation processes of phospholipids as suggested by Hsu and Turk[145] result in a loss of the head group ($(OH)_2POOX$) with product ions ($[M+H-(OH)_2POOX]^+$) that were observed also in here, see also Table 1. Further fragmentation of these ions may result in the formation of $[FA+26]^+$ species.

9 REFERENCES

1. World Health Organization. Antimicrobial resistance: global report on surveillance. 2014. Available from: http://www.who.int/drugresistance/documents/surveillancereport/en.
2. Fair, R. J.; Tor, Y. Antibiotics and Bacterial Resistance in the 21st Century. *Perspectives in Medicinal Chemistry* **2014,** 6, 25-64.
3. World Health Organization. Global Action Plan on Antimicrobial Resistance. 2015 Available from: http://apps.who.int/iris/bitstream/10665/193736/1/9789241509763_eng.pdf.
4. Blair, J. M.; Webber, M. A.; Baylay, A. J.; Ogbolu, D. O.; Piddock, L. J. Molecular mechanisms of antibiotic resistance. *Nat Rev Microbiol* **2015,** 13, 42-51.
5. Rasko, D. A.; Sperandio, V. Anti-virulence strategies to combat bacteria-mediated disease. *Nat Rev Drug Discov* **2010,** 9, 117-128.
6. Davies, J.; Davies, D. Origins and Evolution of Antibiotic Resistance. *Microbiology and Molecular Biology Reviews : MMBR* **2010,** 74, 417-433.
7. D/'Costa, V. M.; King, C. E.; Kalan, L.; Morar, M.; Sung, W. W. L.; Schwarz, C.; Froese, D.; Zazula, G.; Calmels, F.; Debruyne, R.; Golding, G. B.; Poinar, H. N.; Wright, G. D. Antibiotic resistance is ancient. *Nature* **2011,** 477, 457-461.
8. European Centre for Disease Prevention and Control. The bacterial challenge: time to react. 2009. Available from: http://www.ecdc.europa.eu/en/publications/Publications/0909_TER_The_Bacterial_Challenge_Time_to_React.pdf.
9. Centers for Disease Control and Prevention. Antibiotic resistance threats in the United States. 2013. Available from: https://www.cdc.gov/drugresistance/pdf/ar-threats-2013-508.pdf.
10. Conly, J. M.; Johnston, B. L. Where are all the new antibiotics? The new antibiotic paradox. *The Canadian Journal of Infectious Diseases & Medical Microbiology* **2005,** 16, 159-160.
11. Brauner, A.; Fridman, O.; Gefen, O.; Balaban, N. Q. Distinguishing between resistance, tolerance and persistence to antibiotic treatment. *Nat Rev Micro* **2016,** 14, 320-330.
12. Kaldalu, N.; Hauryliuk, V.; Tenson, T. Persisters—as elusive as ever. *Applied Microbiology and Biotechnology* **2016**, 1-9.
13. Magnusson, L. U.; Farewell, A.; Nyström, T. ppGpp: a global regulator in Escherichia coli. *Trends in Microbiology* **2005,** 13, 236-242.
14. Tuchscherr, L.; Medina, E.; Hussain, M.; Völker, W.; Heitmann, V.; Niemann, S.; Holzinger, D.; Roth, J.; Proctor, R. A.; Becker, K.; Peters, G.; Löffler, B. Staphylococcus aureus phenotype switching: an effective bacterial strategy to escape host immune response and establish a chronic infection. *EMBO Molecular Medicine* **2011,** 3, 129-141.
15. Heraud, P.; Wood, B. R.; Beardall, J.; McNaughton, D. Effects of pre-processing of Raman spectra on in vivo classification of nutrient status of microalgal cells. *Journal of Chemometrics* **2006,** 20, 193-197.
16. Gerdes, K.; Ingmer, H. Antibiotics: Killing the survivors. *Nature* **2013,** 503, 347-349.
17. Balaban, N. Q.; Merrin, J.; Chait, R.; Kowalik, L.; Leibler, S. Bacterial Persistence as a Phenotypic Switch. *Science* **2004,** 305, 1622-1625.
18. El Meouche, I.; Siu, Y.; Dunlop, M. J. Stochastic expression of a multiple antibiotic resistance activator confers transient resistance in single cells. *Scientific Reports* **2016,** 6, 19538.
19. Wood, T. K. Combatting bacterial persister cells. *Biotechnol Bioeng* **2016,** 113, 476-83.
20. Gerdes, K.; Maisonneuve, E. Bacterial persistence and toxin-antitoxin loci. *Annu Rev Microbiol* **2012,** 66, 103-23.
21. Page, R.; Peti, W. Toxin-antitoxin systems in bacterial growth arrest and persistence. *Nat Chem Biol* **2016,** 12, 208-214.
22. Maisonneuve, E.; Gerdes, K. Molecular Mechanisms Underlying Bacterial Persisters. *Cell* **2014,** 157, 539-548.
23. Escaich, S. Antivirulence as a new antibacterial approach for chemotherapy. *Current Opinion in Chemical Biology* **2008,** 12, 400-408.
24. Cegelski, L.; Marshall, G. R.; Eldridge, G. R.; Hultgren, S. J. The biology and future prospects of antivirulence therapies. *Nat Rev Micro* **2008,** 6, 17-27.
25. Casadevall, A.; Pirofski, L. a. Host-Pathogen Interactions: The Attributes of Virulence. *Journal of Infectious Diseases* **2001,** 184, 337-344.

26. Andersson, D. I.; Hughes, D. Microbiological effects of sublethal levels of antibiotics. *Nat Rev Micro* **2014,** 12, 465-478.
27. Proft, T.; Baker, E. N. Pili in Gram-negative and Gram-positive bacteria — structure, assembly and their role in disease. *Cellular and Molecular Life Sciences* **2009,** 66, 613-635.
28. Thanassi, D. G.; Bliska, J. B.; Christie, P. J. Surface Organelles Assembled by Secretion Systems of Gram-Negative Bacteria: Diversity in Structure and Function. *FEMS microbiology reviews* **2012,** 36, 1046-1082.
29. Muhlen, S.; Dersch, P. Anti-virulence Strategies to Target Bacterial Infections. *Curr Top Microbiol Immunol* **2016**.
30. Foster, T. J.; Geoghegan, J. A.; Ganesh, V. K.; Hook, M. Adhesion, invasion and evasion: the many functions of the surface proteins of Staphylococcus aureus. *Nat Rev Micro* **2014,** 12, 49-62.
31. Hendrickx, A. P.; Willems, R. J.; Bonten, M. J.; van Schaik, W. LPxTG surface proteins of enterococci. *Trends Microbiol* **2009,** 17, 423-30.
32. Krachler, A. M.; Orth, K. Targeting the bacteria–host interface: Strategies in anti-adhesion therapy. *Virulence* **2013,** 4, 284-294.
33. Maresso, A. W.; Schneewind, O. Sortase as a target of anti-infective therapy. *Pharmacol Rev* **2008,** 60, 128-41.
34. Melvin, J. A.; Murphy, C. F.; Dubois, L. G.; Thompson, J. W.; Moseley, M. A.; McCafferty, D. G. Staphylococcus aureus Sortase A Contributes to the Trojan Horse Mechanism of Immune Defense Evasion with Its Intrinsic Resistance to Cys184 Oxidation. *Biochemistry* **2011,** 50, 7591-7599.
35. Pinkner, J. S.; Remaut, H.; Buelens, F.; Miller, E.; Aberg, V.; Pemberton, N.; Hedenstrom, M.; Larsson, A.; Seed, P.; Waksman, G.; Hultgren, S. J.; Almqvist, F. Rationally designed small compounds inhibit pilus biogenesis in uropathogenic bacteria. *Proc Natl Acad Sci U S A* **2006,** 103, 17897-902.
36. Römling, U.; Balsalobre, C. Biofilm infections, their resilience to therapy and innovative treatment strategies. *Journal of Internal Medicine* **2012,** 272, 541-561.
37. Rutherford, S. T.; Bassler, B. L. Bacterial quorum sensing: its role in virulence and possibilities for its control. *Cold Spring Harb Perspect Med* **2012,** 2.
38. Gooderham, W. J.; Hancock, R. E. W. Regulation of virulence and antibiotic resistance by two-component regulatory systems in Pseudomonas aeruginosa. *FEMS Microbiology Reviews* **2009,** 33, 279-294.
39. Clatworthy, A. E.; Pierson, E.; Hung, D. T. Targeting virulence: a new paradigm for antimicrobial therapy. *Nat Chem Biol* **2007,** 3, 541-8.
40. Hentzer, M.; Wu, H.; Andersen, J. B.; Riedel, K.; Rasmussen, T. B.; Bagge, N.; Kumar, N.; Schembri, M. A.; Song, Z.; Kristoffersen, P.; Manefield, M.; Costerton, J. W.; Molin, S.; Eberl, L.; Steinberg, P.; Kjelleberg, S.; Høiby, N.; Givskov, M. Attenuation of Pseudomonas aeruginosa virulence by quorum sensing inhibitors. *The EMBO Journal* **2003,** 22, 3803-3815.
41. Mansson, M.; Nielsen, A.; Kjærulff, L.; Gotfredsen, C. H.; Wietz, M.; Ingmer, H.; Gram, L.; Larsen, T. O. Inhibition of Virulence Gene Expression in Staphylococcus aureus by Novel Depsipeptides from a Marine Photobacterium. *Marine Drugs* **2011,** 9, 2537.
42. Nielsen, A.; Månsson, M.; Bojer, M. S.; Gram, L.; Larsen, T. O.; Novick, R. P.; Frees, D.; Frøkiær, H.; Ingmer, H. Solonamide B Inhibits Quorum Sensing and Reduces Staphylococcus aureus Mediated Killing of Human Neutrophils. *PLoS ONE* **2014,** 9, e84992.
43. Dong, T. G.; Ho, B. T.; Yoder-Himes, D. R.; Mekalanos, J. J. Identification of T6SS-dependent effector and immunity proteins by Tn-seq in Vibrio cholerae. *Proceedings of the National Academy of Sciences of the United States of America* **2013,** 110, 2623-2628.
44. Wiles, T. J.; Mulvey, M. A. The RTX pore-forming toxin α-hemolysin of uropathogenic Escherichia coli: progress and perspectives. *Future microbiology* **2013,** 8, 73-84.
45. Henkel, J. S.; Baldwin, M. R.; Barbieri, J. T. Toxins from Bacteria. *EXS* **2010,** 100, 1-29.
46. Liu, S.; Zhang, Y.; Moayeri, M.; Liu, J.; Crown, D.; Fattah, R. J.; Wein, A. N.; Yu, Z.-X.; Finkel, T.; Leppla, S. H. Key tissue targets responsible for anthrax-toxin-induced lethality. *Nature* **2013,** 501, 63-68.
47. Peraro, M. D.; van der Goot, F. G. Pore-forming toxins: ancient, but never really out of fashion. *Nat Rev Micro* **2016,** 14, 77-92.
48. Keyser, P.; Elofsson, M.; Rosell, S.; Wolf-Watz, H. Virulence blockers as alternatives to antibiotics: type III secretion inhibitors against Gram-negative bacteria. *Journal of Internal Medicine* **2008,** 264, 17-29.
49. Hauser, A. R.; Mecsas, J.; Moir, D. T. Beyond Antibiotics: New Therapeutic Approaches for Bacterial Infections. *Clinical Infectious Diseases* **2016,** 63, 89-95.

50. Kimura, K.; Iwatsuki, M.; Nagai, T.; Matsumoto, A.; Takahashi, Y.; Shiomi, K.; Omura, S.; Abe, A. A small-molecule inhibitor of the bacterial type III secretion system protects against in vivo infection with Citrobacter rodentium. *J Antibiot* **2011,** 64, 197-203.
51. Hung, D. T.; Shakhnovich, E. A.; Pierson, E.; Mekalanos, J. J. Small-molecule inhibitor of Vibrio cholerae virulence and intestinal colonization. *Science* **2005,** 310, 670-4.
52. Sintchenko, V.; Iredell, J. R.; Gilbert, G. L. Pathogen profiling for disease management and surveillance. *Nat Rev Micro* **2007,** 5, 464-470.
53. Garcia-Contreras, R.; Nunez-Lopez, L.; Jasso-Chavez, R.; Kwan, B. W.; Belmont, J. A.; Rangel-Vega, A.; Maeda, T.; Wood, T. K. Quorum sensing enhancement of the stress response promotes resistance to quorum quenching and prevents social cheating. *ISME J* **2015,** 9, 115-125.
54. Lina, G.; Piémont, Y.; Godail-Gamot, F.; Bes, M.; Peter, M.-O.; Gauduchon, V.; Vandenesch, F.; Etienne, J. Involvement of Panton-Valentine Leukocidin—Producing Staphylococcus aureus in Primary Skin Infections and Pneumonia. *Clinical Infectious Diseases* **1999,** 29, 1128-1132.
55. Mazmanian, S. K.; Liu, G.; Ton-That, H.; Schneewind, O. Staphylococcus aureus Sortase, an Enzyme that Anchors Surface Proteins to the Cell Wall. *Science* **1999,** 285, 760-763.
56. Mazmanian, S. K.; Liu, G.; Jensen, E. R.; Lenoy, E.; Schneewind, O. Staphylococcus aureus sortase mutants defective in the display of surface proteins and in the pathogenesis of animal infections. *Proceedings of the National Academy of Sciences of the United States of America* **2000,** 97, 5510-5515.
57. Hendrickx, A. P. A.; Budzik, J. M.; Oh, S.-Y.; Schneewind, O. Architects at the bacterial surface — sortases and the assembly of pili with isopeptide bonds. *Nat Rev Micro* **2011,** 9, 166-176.
58. Pallen, M. J.; Lam, A. C.; Antonio, M.; Dunbar, K. An embarrassment of sortases – a richness of substrates? *Trends in Microbiology* **2001,** 9, 97-101.
59. Breukink, E.; de Kruijff, B. Lipid II as a target for antibiotics. *Nat Rev Drug Discov* **2006,** 5, 321-323.
60. Suree, N.; Liew, C. K.; Villareal, V. A.; Thieu, W.; Fadeev, E. A.; Clemens, J. J.; Jung, M. E.; Clubb, R. T. The Structure of the Staphylococcus aureus Sortase-Substrate Complex Reveals How the Universally Conserved LPXTG Sorting Signal Is Recognized. *Journal of Biological Chemistry* **2009,** 284, 24465-24477.
61. Cascioferro, S.; Totsika, M.; Schillaci, D. Sortase A: An ideal target for anti-virulence drug development. *Microbial Pathogenesis* **2014,** 77, 105-112.
62. Guo, Y.; Cai, S.; Gu, G.; Guo, Z.; Long, Z. Recent progress in the development of sortase A inhibitors as novel anti-bacterial virulence agents. *RSC Advances* **2015,** 5, 49880-49889.
63. Weiss, W. J.; Lenoy, E.; Murphy, T.; Tardio, L.; Burgio, P.; Projan, S. J.; Schneewind, O.; Alksne, L. Effect of srtA and srtB gene expression on the virulence of Staphylococcus aureus in animal models of infection. *Journal of Antimicrobial Chemotherapy* **2004,** 53, 480-486.
64. Kubica, M.; Guzik, K.; Koziel, J.; Zarebski, M.; Richter, W.; Gajkowska, B.; Golda, A.; Maciag-Gudowska, A.; Brix, K.; Shaw, L.; Foster, T.; Potempa, J. A Potential New Pathway for <italic>Staphylococcus aureus</italic> Dissemination: The Silent Survival of <italic>S. aureus</italic> Phagocytosed by Human Monocyte-Derived Macrophages. *PLoS ONE* **2008,** 3, e1409.
65. Bierne, H.; Mazmanian, S. K.; Trost, M.; Pucciarelli, M. G.; Liu, G.; Dehoux, P.; Jansch, L.; Garcia-del Portillo, F.; Schneewind, O.; Cossart, P. Inactivation of the srtA gene in Listeria monocytogenes inhibits anchoring of surface proteins and affects virulence. *Mol Microbiol* **2002,** 43, 869-81.
66. Garandeau, C.; Reglier-Poupet, H.; Dubail, I.; Beretti, J. L.; Berche, P.; Charbit, A. The sortase SrtA of Listeria monocytogenes is involved in processing of internalin and in virulence. *Infect Immun* **2002,** 70, 1382-90.
67. Kharat, A. S.; Tomasz, A. Inactivation of the srtA gene affects localization of surface proteins and decreases adhesion of Streptococcus pneumoniae to human pharyngeal cells in vitro. *Infect Immun* **2003,** 71, 2758-65.
68. Vanier, G.; Sekizaki, T.; Dominguez-Punaro, M. C.; Esgleas, M.; Osaki, M.; Takamatsu, D.; Segura, M.; Gottschalk, M. Disruption of srtA gene in Streptococcus suis results in decreased interactions with endothelial cells and extracellular matrix proteins. *Vet Microbiol* **2008,** 127, 417-24.
69. Wang, L.; Bi, C.; Cai, H.; Liu, B.; Zhong, X.; Deng, X.; Wang, T.; Xiang, H.; Niu, X.; Wang, D. The therapeutic effect of chlorogenic acid against Staphylococcus aureus infection through sortase A inhibition. *Frontiers in Microbiology* **2015,** 6, 1031.
70. Zhang, J.; Liu, H.; Zhu, K.; Gong, S.; Dramsi, S.; Wang, Y.-T.; Li, J.; Chen, F.; Zhang, R.; Zhou, L.; Lan, L.; Jiang, H.; Schneewind, O.; Luo, C.; Yang, C.-G. Antiinfective therapy with a small molecule inhibitor of Staphylococcus aureus sortase. *Proceedings of the National Academy of Sciences of the United States of America* **2014,** 111, 13517-13522.

71. Cascioferro, S.; Raffa, D.; Maggio, B.; Raimondi, M. V.; Schillaci, D.; Daidone, G. Sortase A Inhibitors: Recent Advances and Future Perspectives. *Journal of Medicinal Chemistry* **2015,** 58, 9108-9123.
72. Kim, S. H.; Shin, D. S.; Oh, M. N.; Chung, S. C.; Lee, J. S.; Chang, I. M.; Oh, K. B. Inhibition of sortase, a bacterial surface protein anchoring transpeptidase, by beta-sitosterol-3-O-glucopyranoside from Fritillaria verticillata. *Biosci Biotechnol Biochem* **2003,** 67, 2477-9.
73. Kim, S. H.; Shin, D. S.; Oh, M. N.; Chung, S. C.; Lee, J. S.; Oh, K. B. Inhibition of the bacterial surface protein anchoring transpeptidase sortase by isoquinoline alkaloids. *Biosci Biotechnol Biochem* **2004,** 68, 421-4.
74. Oh, K.-B.; Mar, W.; Kim, S.; Kim, J.-Y.; Oh, M.-N.; Kim, J.-G.; Shin, D.; Sim, C. J.; Shin, J. Bis(indole) alkaloids as sortase A inhibitors from the sponge Spongosorites sp. *Bioorganic & Medicinal Chemistry Letters* **2005,** 15, 4927-4931.
75. Jang, K. H.; Chung, S. C.; Shin, J.; Lee, S. H.; Kim, T. I.; Lee, H. S.; Oh, K. B. Aaptamines as sortase A inhibitors from the tropical sponge Aaptos aaptos. *Bioorg Med Chem Lett* **2007,** 17, 5366-9.
76. Park, B. S.; Kim, J. G.; Kim, M. R.; Lee, S. E.; Takeoka, G. R.; Oh, K. B.; Kim, J. H. Curcuma longa L. constituents inhibit sortase A and Staphylococcus aureus cell adhesion to fibronectin. *J Agric Food Chem* **2005,** 53, 9005-9.
77. Lee, S.; Song, I. H.; Lee, J. H.; Yang, W. Y.; Oh, K. B.; Shin, J. Sortase A inhibitory metabolites from the roots of Pulsatilla koreana. *Bioorg Med Chem Lett* **2014,** 24, 44-8.
78. Huang, P.; Hu, P.; Zhou, S. Y.; Li, Q.; Chen, W. M. Morin inhibits sortase A and subsequent biofilm formation in Streptococcus mutans. *Curr Microbiol* **2014,** 68, 47-52.
79. Liu, B.; Chen, F.; Bi, C.; Wang, L.; Zhong, X.; Cai, H.; Deng, X.; Niu, X.; Wang, D. Quercitrin, an inhibitor of Sortase A, interferes with the adhesion of Staphylococcal aureus. *Molecules* **2015,** 20, 6533-43.
80. Oh, I.; Yang, W. Y.; Chung, S. C.; Kim, T. Y.; Oh, K. B.; Shin, J. In vitro sortase A inhibitory and antimicrobial activity of flavonoids isolated from the roots of Sophora flavescens. *Arch Pharm Res* **2011,** 34, 217-22.
81. Yang, W. Y.; Kim, C. K.; Ahn, C. H.; Kim, H.; Shin, J.; Oh, K. B. Flavonoid Glycosides Inhibit Sortase A and Sortase A-Mediated Aggregation of Streptococcus mutans, an Oral Bacterium Responsible for Human Dental Caries. *J Microbiol Biotechnol* **2016**.
82. Wallock-Richards, D. J.; Marles-Wright, J.; Clarke, D. J.; Maitra, A.; Dodds, M.; Hanley, B.; Campopiano, D. J. Molecular basis of Streptococcus mutans sortase A inhibition by the flavonoid natural product trans-chalcone. *Chem Commun (Camb)* **2015,** 51, 10483-5.
83. Lee, Y. J.; Han, Y. R.; Park, W.; Nam, S. H.; Oh, K. B.; Lee, H. S. Synthetic analogs of indole-containing natural products as inhibitors of sortase A and isocitrate lyase. *Bioorg Med Chem Lett* **2010,** 20, 6882-5.
84. Oh, K.-B.; Kim, S.-H.; Lee, J.; Cho, W.-J.; Lee, T.; Kim, S. Discovery of Diarylacrylonitriles as a Novel Series of Small Molecule Sortase A Inhibitors. *Journal of Medicinal Chemistry* **2004,** 47, 2418-2421.
85. Maresso, A. W.; Wu, R.; Kern, J. W.; Zhang, R.; Janik, D.; Missiakas, D. M.; Duban, M.-E.; Joachimiak, A.; Schneewind, O. Activation of Inhibitors by Sortase Triggers Irreversible Modification of the Active Site. *Journal of Biological Chemistry* **2007,** 282, 23129-23139.
86. Suree, N.; Yi, S. W.; Thieu, W.; Marohn, M.; Damoiseaux, R.; Chan, A.; Jung, M. E.; Clubb, R. T. Discovery and structure–activity relationship analysis of Staphylococcus aureus sortase A inhibitors. *Bioorganic & medicinal chemistry* **2009,** 17, 7174-7185.
87. Zhulenkovs, D.; Rudevica, Z.; Jaudzems, K.; Turks, M.; Leonchiks, A. Discovery and structure–activity relationship studies of irreversible benzisothiazolinone-based inhibitors against Staphylococcus aureus sortase A transpeptidase. *Bioorganic & Medicinal Chemistry* **2014,** 22, 5988-6003.
88. Rentero Rebollo, I.; McCallin, S.; Bertoldo, D.; Entenza, J. M.; Moreillon, P.; Heinis, C. Development of Potent and Selective S. aureus Sortase A Inhibitors Based on Peptide Macrocycles. *ACS Medicinal Chemistry Letters* **2016**.
89. Maggio, B.; Raffa, D.; Raimondi, M.; Cascioferro, S.; Plescia, F.; Schillaci, D.; Cusimano, M.; Leonchiks, A.; Zhulenkovs, D.; Basile, L.; Daidone, G. Discovery of a New Class of Sortase A Transpeptidase Inhibitors to Tackle Gram-Positive Pathogens: 2-(2-Phenylhydrazinylidene)alkanoic Acids and Related Derivatives. *Molecules* **2016,** 21, 241.
90. Boute, N.; Jockers, R.; Issad, T. The use of resonance energy transfer in high-throughput screening: BRET versus FRET. *Trends in Pharmacological Sciences* **2002,** 23, 351-354.

91. Sapsford, K. E.; Berti, L.; Medintz, I. L. Materials for Fluorescence Resonance Energy Transfer Analysis: Beyond Traditional Donor–Acceptor Combinations. *Angewandte Chemie International Edition* **2006,** 45, 4562-4589.
92. Meiboom, S.; Gill, D. Modified Spin-Echo Method for Measuring Nuclear Relaxation Times. *Review of Scientific Instruments* **1958,** 29, 688-691.
93. Kleckner, I. R.; Foster, M. P. An introduction to NMR-based approaches for measuring protein dynamics. *Biochimica et biophysica acta* **2011,** 1814, 942-968.
94. Hajduk, P. J.; Olejniczak, E. T.; Fesik, S. W. One-Dimensional Relaxation- and Diffusion-Edited NMR Methods for Screening Compounds That Bind to Macromolecules. *Journal of the American Chemical Society* **1997,** 119, 12257-12261.
95. Patching, S. G. Surface plasmon resonance spectroscopy for characterisation of membrane protein–ligand interactions and its potential for drug discovery. *Biochimica et Biophysica Acta (BBA) - Biomembranes* **2014,** 1838, 43-55.
96. Cooper, M. A. Optical biosensors in drug discovery. *Nat Rev Drug Discov* **2002,** 1, 515-528.
97. Harz, M.; Rösch, P.; Popp, J. Vibrational spectroscopy—A powerful tool for the rapid identification of microbial cells at the single-cell level. *Cytometry Part A* **2009,** 75A, 104-113.
98. Becker, K.; Laham, N. A.; Fegeler, W.; Proctor, R. A.; Peters, G.; von Eiff, C. Fourier-Transform Infrared Spectroscopic Analysis Is a Powerful Tool for Studying the Dynamic Changes in Staphylococcus aureus Small-Colony Variants. *Journal of Clinical Microbiology* **2006,** 44, 3274-3278.
99. Preisner, O.; Lopes, J. A.; Guiomar, R.; Machado, J.; Menezes, J. C. Fourier transform infrared (FT-IR) spectroscopy in bacteriology: towards a reference method for bacteria discrimination. *Analytical and Bioanalytical Chemistry* **2007,** 387, 1739-1748.
100. Whittaker, P.; Mossoba, M. M.; Al-Khaldi, S.; Fry, F. S.; Dunkel, V. C.; Tall, B. D.; Yurawecz, M. P. Identification of foodborne bacteria by infrared spectroscopy using cellular fatty acid methyl esters. *Journal of Microbiological Methods* **2003,** 55, 709-716.
101. Davis, R.; Mauer, L. J. Fourier tansform infrared (FT-IR) spectroscopy: A rapid tool for
detection and analysis of foodborne pathogenic bacteria. *Current research, technology and education topics in applied microbiology and microbial biotechnology, A. Mendez-Vilas (Ed.) Formatex Research Center* **2010,** 2, 1582-1594.
102. Lundstedt, T.; Seifert, E.; Abramo, L.; Thelin, B.; Nyström, Å.; Pettersen, J.; Bergman, R. Experimental design and optimization. *Chemometrics and Intelligent Laboratory Systems* **1998,** 42, 3-40.
103. Shaffer, R. E. Multi- and Megavariate Data Analysis. Principles and Applications, I. Eriksson, E. Johansson, N. Kettaneh-Wold and S. Wold, Umetrics Academy, Umeå, 2001, ISBN 91-973730-1-X, 533pp. *Journal of Chemometrics* **2002,** 16, 261-262.
104. Rinnan, Å.; Berg, F. v. d.; Engelsen, S. B. Review of the most common pre-processing techniques for near-infrared spectra. *TrAC Trends in Analytical Chemistry* **2009,** 28, 1201-1222.
105. Martens, H.; Bruun, S. W.; Adt, I.; Sockalingum, G. D.; Kohler, A. Pre-processing in biochemometrics: correction for path-length and temperature effects of water in FTIR bio-spectroscopy by EMSC. *Journal of Chemometrics* **2006,** 20, 402-417.
106. Wold, S. Cross-Validatory Estimation of the Number of Components in Factor and Principal Components Models. *Technometrics* **1978,** 20, 397-405.
107. Trygg, J.; Wold, S. Orthogonal projections to latent structures (O-PLS). *Journal of Chemometrics* **2002,** 16, 119-128.
108. Crompton, M. J.; Dunstan, R. H.; Macdonald, M. M.; Gottfries, J.; von Eiff, C.; Roberts, T. K. Small Changes in Environmental Parameters Lead to Alterations in Antibiotic Resistance, Cell Morphology and Membrane Fatty Acid Composition in <italic>Staphylococcus lugdunensis</italic>. *PLoS ONE* **2014,** 9, e92296.
109. Naumann, D. FT-INFRARED AND FT-RAMAN SPECTROSCOPY IN BIOMEDICAL RESEARCH. *Applied Spectroscopy Reviews* **2001,** 36, 239-298.
110. Oprea, T. I.; Gottfries, J. Chemography: The Art of Navigating in Chemical Space. *Journal of Combinatorial Chemistry* **2001,** 3, 157-166.
111. Fletcher, J. S.; Vickerman, J. C.; Winograd, N. Label free biochemical 2D and 3D imaging using secondary ion mass spectrometry. *Current opinion in chemical biology* **2011,** 15, 733-740.
112. Davies, N.; Weibel, D. E.; Blenkinsopp, P.; Lockyer, N.; Hill, R.; Vickerman, J. C. Development and experimental application of a gold liquid metal ion source. *Applied Surface Science* **2003,** 203–204, 223-227.

113. Touboul, D.; Kollmer, F.; Niehuis, E.; Brunelle, A.; Laprévote, O. Improvement of biological time-of-flight-secondary ion mass spectrometry imaging with a bismuth cluster ion source. *Journal of the American Society for Mass Spectrometry* **2005,** 16, 1608-1618.
114. Kötter, F.; Benninghoven, A. Secondary ion emission from polymer surfaces under Ar+, Xe+ and SF5+ ion bombardment. *Applied Surface Science* **1998,** 133, 47-57.
115. Weibel, D.; Wong, S.; Lockyer, N.; Blenkinsopp, P.; Hill, R.; Vickerman, J. C. A C60 Primary Ion Beam System for Time of Flight Secondary Ion Mass Spectrometry: Its Development and Secondary Ion Yield Characteristics. *Analytical Chemistry* **2003,** 75, 1754-1764.
116. Ninomiya, S.; Nakata, Y.; Honda, Y.; Ichiki, K.; Seki, T.; Aoki, T.; Matsuo, J. A fragment-free ionization technique for organic mass spectrometry with large Ar cluster ions. *Applied Surface Science* **2008,** 255, 1588-1590.
117. Yamada, I.; Matsuo, J.; Toyoda, N.; Kirkpatrick, A. Materials processing by gas cluster ion beams. *Materials Science and Engineering: R: Reports* **2001,** 34.
118. Angerer, T. B.; Blenkinsopp, P.; Fletcher, J. S. High energy gas cluster ions for organic and biological analysis by time-of-flight secondary ion mass spectrometry. *International Journal of Mass Spectrometry* **2015,** 377, 591-598.
119. Passarelli, M. K.; Winograd, N. Lipid imaging with time-of-flight secondary ion mass spectrometry (ToF-SIMS). *Biochimica et Biophysica Acta (BBA) - Molecular and Cell Biology of Lipids* **2011,** 1811, 976-990.
120. Wehrli, P. M.; Lindberg, E.; Angerer, T. B.; Wold, A. E.; Gottfries, J.; Fletcher, J. S. Maximising the potential for bacterial phenotyping using time-of-flight secondary ion mass spectrometry with multivariate analysis and Tandem Mass Spectrometry. *Surface and Interface Analysis* **2014,** 46, 173-176.
121. Fletcher, J. S.; Henderson, A.; Jarvis, R. M.; Lockyer, N. P.; Vickerman, J. C.; Goodacre, R. Rapid discrimination of the causal agents of urinary tract infection using ToF-SIMS with chemometric cluster analysis. *Applied Surface Science* **2006,** 252, 6869-6874.
122. Lanni, E. J.; Masyuko, R. N.; Driscoll, C. M.; Aerts, J. T.; Shrout, J. D.; Bohn, P. W.; Sweedler, J. V. MALDI-guided SIMS: Multiscale Imaging of Metabolites in Bacterial Biofilms. *Analytical Chemistry* **2014,** 86, 9139-9145.
123. Vaidyanathan, S.; Fletcher, J. S.; Lockyer, N. P.; Vickerman, J. C. TOF-SIMS investigation of Streptomyces coelicolor, a mycelial bacterium. *Applied Surface Science* **2008,** 255, 922-925.
124. Thompson, C. E.; Ellis, J.; Fletcher, J. S.; Goodacre, R.; Henderson, A.; Lockyer, N. P.; Vickerman, J. C. ToF-SIMS studies of Bacillus using multivariate analysis with possible identification and taxonomic applications. *Applied Surface Science* **2006,** 252, 6719-6722.
125. Fletcher, J. S.; Kotze, H. L.; Armitage, E. G.; Lockyer, N. P.; Vickerman, J. C. Evaluating the challenges associated with time-of-fight secondary ion mass spectrometry for metabolomics using pure and mixed metabolites. *Metabolomics* **2013,** 9, 535-544.
126. Fletcher, J. S.; Rabbani, S.; Henderson, A.; Blenkinsopp, P.; Thompson, S. P.; Lockyer, N. P.; Vickerman, J. C. A New Dynamic in Mass Spectral Imaging of Single Biological Cells. *Analytical Chemistry* **2008,** 80, 9058-9064.
127. Åberg, K. M.; Alm, E.; Torgrip, R. J. O. The correspondence problem for metabonomics datasets. *Analytical and Bioanalytical Chemistry* **2009,** 394, 151-162.
128. Lépine, F.; Milot, S.; Déziel, E.; He, J.; Rahme, L. G. Electrospray/mass spectrometric identification and analysis of 4-hydroxy-2-alkylquinolines (HAQs) produced by Pseudomonas aeruginosa. *Journal of the American Society for Mass Spectrometry* **2004,** 15, 862-869.
129. Poole, K. Bacterial stress responses as determinants of antimicrobial resistance. *Journal of Antimicrobial Chemotherapy* **2012**.
130. Chung, H. J.; Bang, W.; Drake, M. A. Stress Response of Escherichia coli. *Comprehensive Reviews in Food Science and Food Safety* **2006,** 5, 52-64.
131. Schenk, E. R.; Nau, F.; Thompson, C. J.; Tse-Dinh, Y.-C.; Fernandez-Lima, F. Changes in lipid distribution in E. coli strains in response to norfloxacin. *Journal of Mass Spectrometry* **2015,** 50, 88-94.
132. Godfrey, H. P.; Bugrysheva, J. V.; Cabello, F. C. The role of the stringent response in the pathogenesis of bacterial infections. *Trends in Microbiology* 10, 349-351.
133. Boutte, C. C.; Crosson, S. Bacterial lifestyle shapes stringent response activation. *Trends in Microbiology* **2013,** 21, 174-180.
134. Janßen, H. J.; Steinbüchel, A. Fatty acid synthesis in Escherichia coli and its applications towards the production of fatty acid based biofuels. *Biotechnology for Biofuels* **2014,** 7, 7-7.
135. Hauryliuk, V.; Atkinson, G. C.; Murakami, K. S.; Tenson, T.; Gerdes, K. Recent functional insights into the role of (p)ppGpp in bacterial physiology. *Nat Rev Micro* **2015,** 13, 298-309.

136. Weber, H.; Polen, T.; Heuveling, J.; Wendisch, V. F.; Hengge, R. Genome-wide analysis of the general stress response network in Escherichia coli: sigmaS-dependent genes, promoters, and sigma factor selectivity. *J Bacteriol* **2005,** 187, 1591-603.
137. Boutte, C. C.; Crosson, S. The complex logic of stringent response regulation in Caulobacter crescentus: starvation signalling in an oligotrophic environment. *Mol Microbiol* **2011,** 80, 695-714.
138. Maisonneuve, E.; Castro-Camargo, M.; Gerdes, K. (p)ppGpp Controls Bacterial Persistence by Stochastic Induction of Toxin-Antitoxin Activity. *Cell* **2013,** 154, 1140-1150.
139. Germain, E.; Castro-Roa, D.; Zenkin, N.; Gerdes, K. Molecular Mechanism of Bacterial Persistence by HipA. *Molecular Cell* **2013,** 52, 248-254.
140. Wexselblatt, E.; Oppenheimer-Shaanan, Y.; Kaspy, I.; London, N.; Schueler-Furman, O.; Yavin, E.; Glaser, G.; Katzhendler, J.; Ben-Yehuda, S. Relacin, a Novel Antibacterial Agent Targeting the Stringent Response. *PLoS Pathog* **2012,** 8, e1002925.
141. Guan, Z.; Li, S.; Smith, D. C.; Shaw, W. A.; Raetz, C. R. H. Identification of N-Acyl Phosphatidylserine Molecules in Eukaryotic Cells. *Biochemistry* **2007,** 46, 14500-14513.
142. Andreazza, H. J.; Wang, T.; Bilusich, D.; Hoffmann, P.; Bowie, J. H. Negative ion fragmentations of deprotonated peptides containing post-translational modifications: diphosphorylated systems containing Ser, Thr and Tyr. A characteristic phosphate/phosphate cyclisation. A joint experimental and theoretical study. *Rapid Communications in Mass Spectrometry* **2009,** 23, 1825-1833.
143. Garrett, T. A.; Raetz, C. R. H.; Richardson, T.; Kordestani, R.; Son, J. D.; Rose, R. L. Identification of phosphatidylserylglutamate: a novel minor lipid in Escherichia coli. *Journal of Lipid Research* **2009,** 50, 1589-1599.
144. Hsu, F.-F.; Turk, J. Differentiation of 1-O-alk-1'-enyl-2-acyl and 1-O-alkyl-2-acyl Glycerolphospholipids by Multiple-stage Linear Ion-trap Mass Spectrometry with Electrospray Ionization. *Journal of the American Society for Mass Spectrometry* **2007,** 18, 2065-2073.
145. Hsu, F.-F.; Turk, J. Electrospray Ionization with Low-energy Collisionally Activated Dissociation Tandem Mass Spectrometry of Glycerophospholipids: Mechanisms of Fragmentation and Structural Characterization. *Journal of chromatography. B, Analytical technologies in the biomedical and life sciences* **2009,** 877, 2673-2695.
146. Rauch, J.; Gumperz, J.; Robinson, C.; Sköld, M.; Roy, C.; Young, D. C.; Lafleur, M.; Moody, D. B.; Brenner, M. B.; Costello, C. E.; Behar, S. M. Structural Features of the Acyl Chain Determine Self-phospholipid Antigen Recognition by a CD1d-restricted Invariant NKT (iNKT) Cell(). *The Journal of biological chemistry* **2003,** 278, 47508-47515.
147. Pulfer, M.; Murphy, R. C. Electrospray mass spectrometry of phospholipids. *Mass Spectrometry Reviews* **2003,** 22, 332-364.
148. Drucker, D. B.; Megson, G.; Harty, D. W.; Riba, I.; Gaskell, S. J. Phospholipids of Lactobacillus spp. *Journal of bacteriology* **1995,** 177, 6304-6308.
149. Oursel, D.; Loutelier-Bourhis, C.; Orange, N.; Chevalier, S.; Norris, V.; Lange, C. M. Lipid composition of membranes of Escherichia coli by liquid chromatography/tandem mass spectrometry using negative electrospray ionization. *Rapid Communications in Mass Spectrometry* **2007,** 21, 1721-1728.
150. Ariöz, C.; Götzke, H.; Lindholm, L.; Eriksson, J.; Edwards, K.; Daley, D. O.; Barth, A.; Wieslander, Å. Heterologous overexpression of a monotopic glucosyltransferase (MGS) induces fatty acid remodeling in Escherichia coli membranes. *Biochimica et Biophysica Acta (BBA) - Biomembranes* **2014,** 1838, 1862-1870.
151. Garrett, T. A.; Raetz, C. R. H.; Son, J. D.; Richardson, T. D.; Bartling, C.; Guan, Z. Non-enzymatically derived minor lipids found in Escherichia coli lipid extracts. *Biochimica et biophysica acta* **2011,** 1811, 827-837.
152. Alves, E.; Santos, N.; Melo, T.; Maciel, E.; Dória, M. L.; Faustino, M. A. F.; Tomé, J. P. C.; Neves, M. G. P. M. S.; Cavaleiro, J. A. S.; Cunha, Â.; Helguero, L. A.; Domingues, P.; Almeida, A.; Domingues, M. R. M. Photodynamic oxidation of Escherichia coli membrane phospholipids: new insights based on lipidomics. *Rapid Communications in Mass Spectrometry* **2013,** 27, 2717-2728.
153. Zhang, Y.-M.; Rock, C. O. Membrane lipid homeostasis in bacteria. *Nat Rev Micro* **2008,** 6, 222-233.
154. Parsons, J. B.; Rock, C. O. Bacterial Lipids: Metabolism and Membrane Homeostasis. *Progress in lipid research* **2013,** 52, 249-276.
155. Chang, Y.-Y.; Cronan, J. E. Membrane cyclopropane fatty acid content is a major factor in acid resistance of Escherichia coli. *Molecular Microbiology* **1999,** 33, 249-259.
156. Tan, B. K.; Bogdanov, M.; Zhao, J.; Dowhan, W.; Raetz, C. R. H.; Guan, Z. Discovery of a cardiolipin synthase utilizing phosphatidylethanolamine and phosphatidylglycerol as substrates. *Proceedings of the National Academy of Sciences* **2012,** 109, 16504-16509.

157. Matsumoto, K.; Hara, H.; Fishov, I.; Mileykovskaya, E.; Norris, V. The Membrane: Transertion as an organizing principle in membrane heterogeneity. *Frontiers in Microbiology* **2015,** 6.
158. Hiraoka, S.; Matsuzaki, H.; Shibuya, I. Active increase in cardiolipin synthesis in the stationary growth phase and its physiological significance in Escherichia coli. *FEBS Letters* **1993,** 336, 221-224.
159. Magnusson, L. U.; Nyström, T.; Farewell, A. Underproduction of ς70 Mimics a Stringent Response: A PROTEOME APPROACH. *Journal of Biological Chemistry* **2003,** 278, 968-973.
160. Chang, D.-E.; Smalley, D. J.; Conway, T. Gene expression profiling of Escherichia coli growth transitions: an expanded stringent response model. *Molecular Microbiology* **2002,** 45, 289-306.
161. Paulucci, N. S.; Dardanelli, M. S.; García de Lema, M. Biochemical and molecular evidence of a Δ9 fatty acid desaturase from Ensifer meliloti 1021. *Microbiological Research* **2014,** 169, 463-468.
162. Farewell, A.; Diez, A. A.; DiRusso, C. C.; Nyström, T. Role of the Escherichia coli FadR regulator in stasis survival and growth phase-dependent expression of the uspA, fad, and fab genes. *Journal of Bacteriology* **1996,** 178, 6443-6450.
163. Traxler, M. F.; Summers, S. M.; Nguyen, H.-T.; Zacharia, V. M.; Smith, J. T.; Conway, T. The global, ppGpp-mediated stringent response to amino acid starvation in Escherichia coli. *Molecular microbiology* **2008,** 68, 1128-1148.
164. Durfee, T.; Hansen, A.-M.; Zhi, H.; Blattner, F. R.; Jin, D. J. Transcription Profiling of the Stringent Response in Escherichia coli. *Journal of Bacteriology* **2008,** 190, 1084-1096.
165. Magnusson, L. U.; Gummesson, B.; Joksimović, P.; Farewell, A.; Nyström, T. Identical, Independent, and Opposing Roles of ppGpp and DksA in Escherichia coli. *Journal of Bacteriology* **2007,** 189, 5193-5202.
166. Laganowsky, A.; Reading, E.; Allison, T. M.; Ulmschneider, M. B.; Degiacomi, M. T.; Baldwin, A. J.; Robinson, C. V. Membrane proteins bind lipids selectively to modulate their structure and function. *Nature* **2014,** 510, 172-175.
167. Lewis, K. Platforms for antibiotic discovery. *Nat Rev Drug Discov* **2013,** 12, 371-387.